Theory and Experiments for Silicon-Based Quantum Computing

SAND2014-19177PE

Malcolm Carroll, Thomas Tarman – Sandia National Labs
{mscarro, tdtarma}@sandia.gov

Objective

- Confine and control single electron spins in silicon nanostructures to form a Si qubit
  - Demonstrate coherent spin control and characterize fidelity
  - Demonstrate donor spin coupling
- Develop supporting theory and technology for present and future silicon qubits and quantum circuitry:
  - Materials characterization, low defect processing and atomic precision fabrication development
  - Device modeling and numeric tool development
  - Integrated fast read-out

Single spin ESR

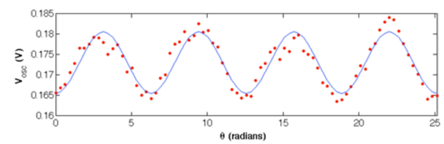

Single Sb^+ ion implant map (50 keV)

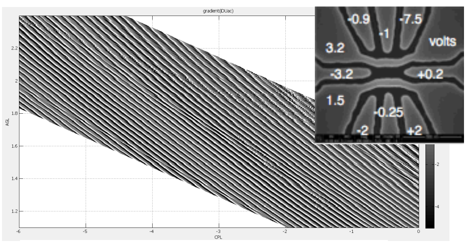

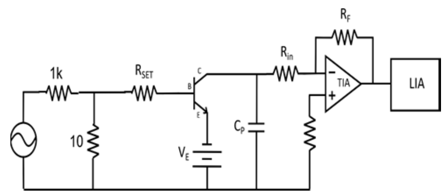

HBT cryogenic amplication

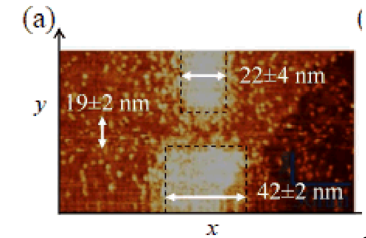

H... ...ces

Objective Approach

- Develop MOS and SiGe/sSi surface gate enhancement mode donor qubit devices to:
  - Demonstrate spin read-out and coherent control
  - Examine self-aligned & vertical structures (e.g., back gated)
- Develop two qubit (donor) structures with either ion implantation or hydrogen lithography assisted fabrication
- Examine cryo-electronics solutions for fast read-out
- Use combinations of numerical packages for multi-scale simulation of quantum dot systems (NEMO3D, EMT, TCAD, SPICE)
- Experimentally determine MOS and SiGe/sSi based donor qubit structures

Status

- B-field dependence & magnitude of T1 consistent with Sb
- ESR bandwidth (~30 GHz) set-up in fridge
- Local ESR line integrated with poly-SET phos. read-out
- Single Sb^{++} ion detection, 50 keV, 100 nm spot in devices with construction zone
- SiGe/sSi gated wire SETs demonstrated & offsets observed in donor implanted devices (possible donor detection in SiGe)
- H-litho on sSOI demonstrated & Ge deposition upgrade
- Completed NEMO calculation of exchange dependence in J-gate configuration

Sandia is a multiprogram laboratory operated by Sandia Corporation, a Lockheed Martin Company, for the United States Department of Energy under Contract No. DE-AC04-94AL85000

Sandia National Laboratories

Theory and Experiments for Silicon-Based Quantum Computing

Malcolm Carroll, Thomas Tarman – Sandia National Labs

Progress on last years objectives

MOS donor devices

Timed implant

- Fabricate: 28Si donor ESR structures & continue to develop ESR & NMR measurements
- Improve fidelity of ESR

Counted implant

- Improved counted ion implant capability (E< 50 keV Sb with 80% DE in construction zone)
- Fabricate J-gate structures
- Correlate number of offsets with counted implant number

Advanced fabrication

Timed implant

- Fabricate: SiGe/sSi gated wires with back plane, implanted donors and ESR capability
- Measure spin read-out of implanted SiGe/sSi SET

H-lithography

- Demonstrate in-plane spin read-out structure on sSOI
- Integrate surface gates with SiGe/sSOI epitaxy

Device modeling & gate error models

- Model effect of strain on spin properties in Si (e.g., T1)
- Develop model for inelastic tunneling between donor and surface dot
- Improve precision and accuracy of models of experimental devices (e.g., triangulation of donors)

Research plan for the next 12 months

- MOS: > 90% gate fidelity in MOS implanted structures
- MOS: demonstrate exchange between two spins
- SiGe/sSi: spin read-out demonstration & ESR integration
- SiGe/sSi: H-litho & SiGe integration with surface gates (e.g., ESR line & A-gate)

Long term objectives (demonstrations)

Develop and measure donor nanostructures for electron spin based silicon multi-qubit systems. Further the understanding of decoherence mechanisms and develop ways to suppress decoherence in these systems. Develop and measure supporting qubit technology (e.g., processing, atomic precision fab., modeling and cryoelectronics) and examine impurity doped quantum dots in a hybrid QD architecture.

Outline

- Motivations
- MOS donor qubits
- Two qubit nanostructures
  - Single ion implant
  - STM
- Summary

Nanostructure fabrication at Sandia National Labs

Front-end in silicon fab

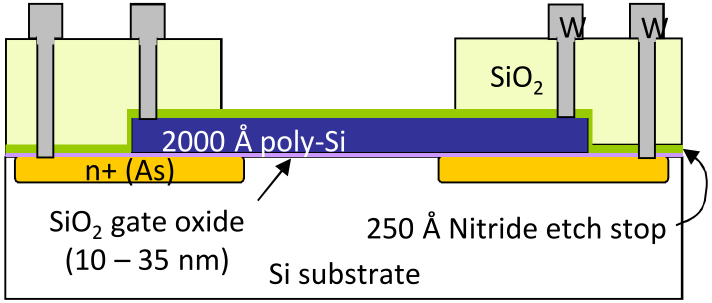

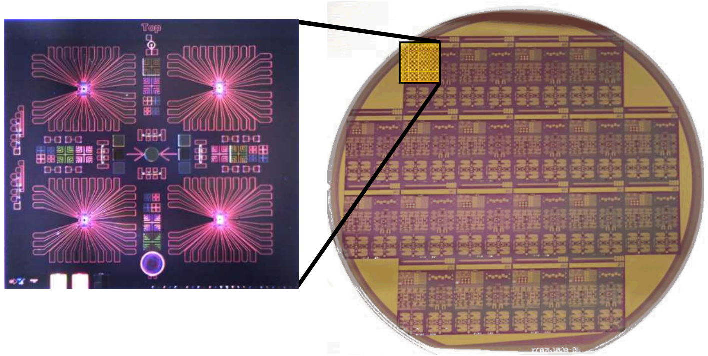

Back-end nanolithography

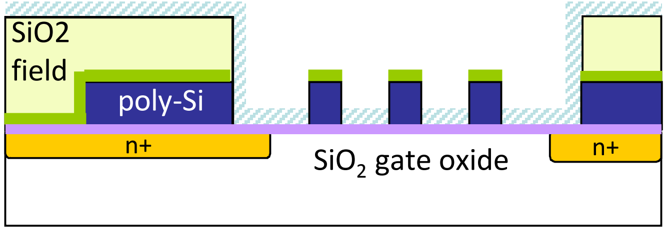

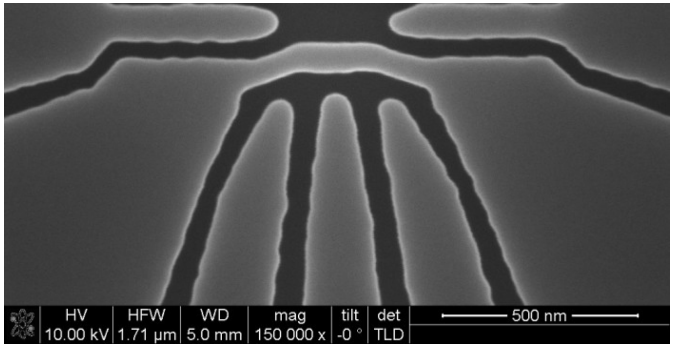

Goal: Use Poly-Si etched structures to produce donor-based qubits

Rationale:

- Self aligned implant
- Foundry like processing

Poly silicon quantum dot

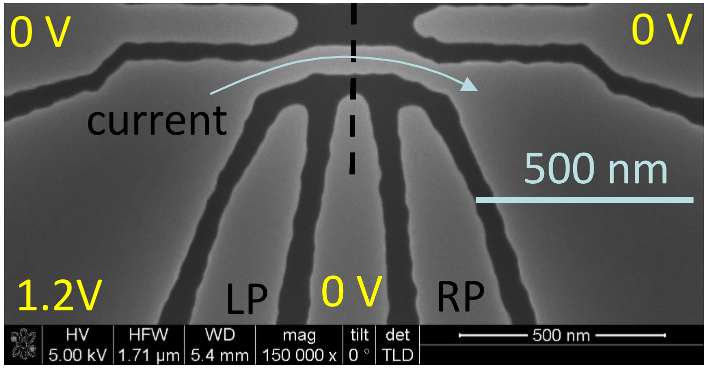

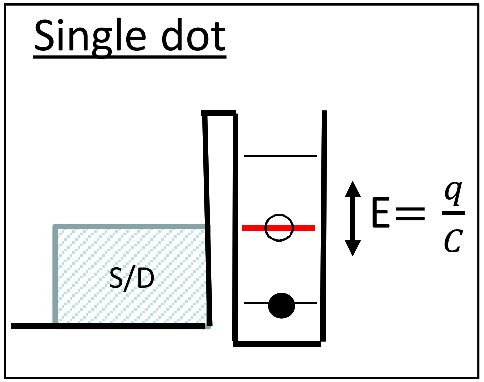

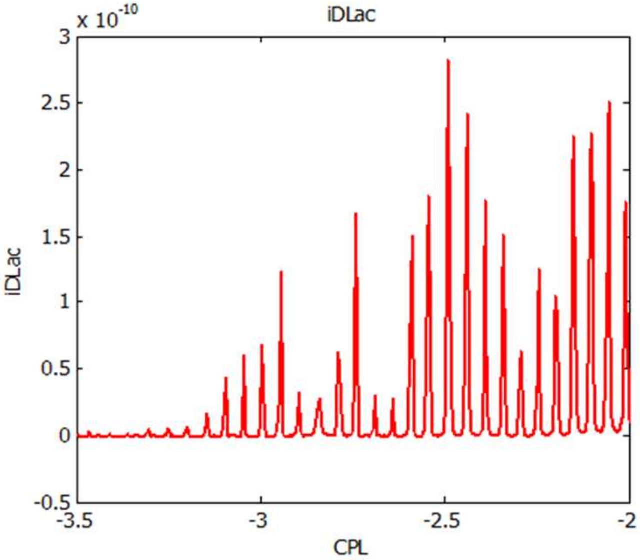

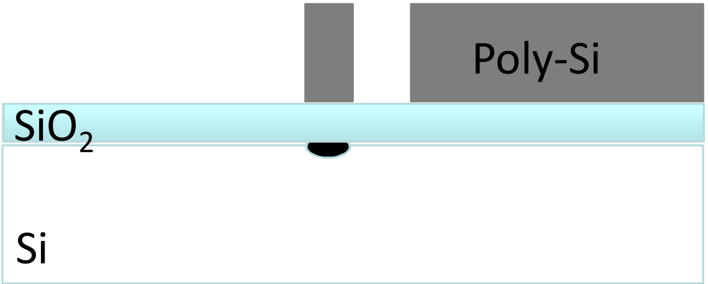

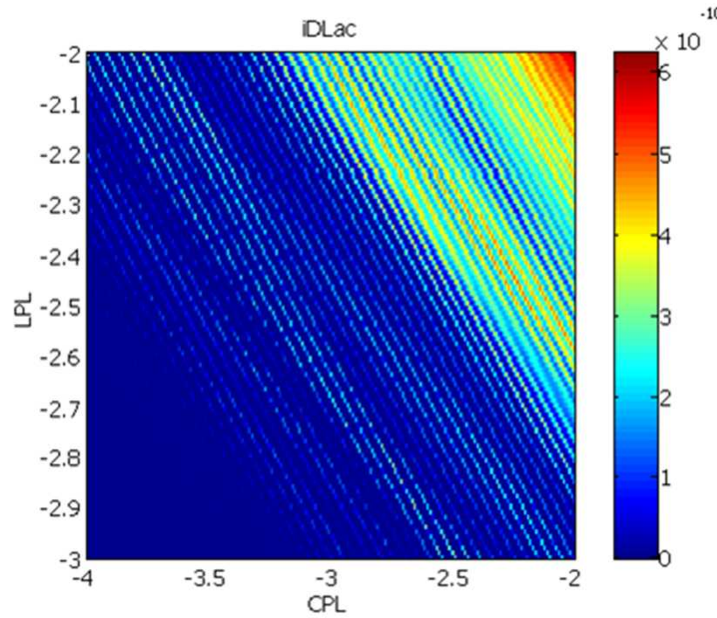

- Simplify SET for donor read-out
  - Implant will be self-aligned
- Relatively regular period Coulomb blockade achieved in poly silicon SET
- Wire width ~50-70 nm with gaps between wire and plunger of ~40-50 nm at tips

Harvey-Collard

Sandia National Laboratories

Semiclassical modelling of lithographic dot

horshidian

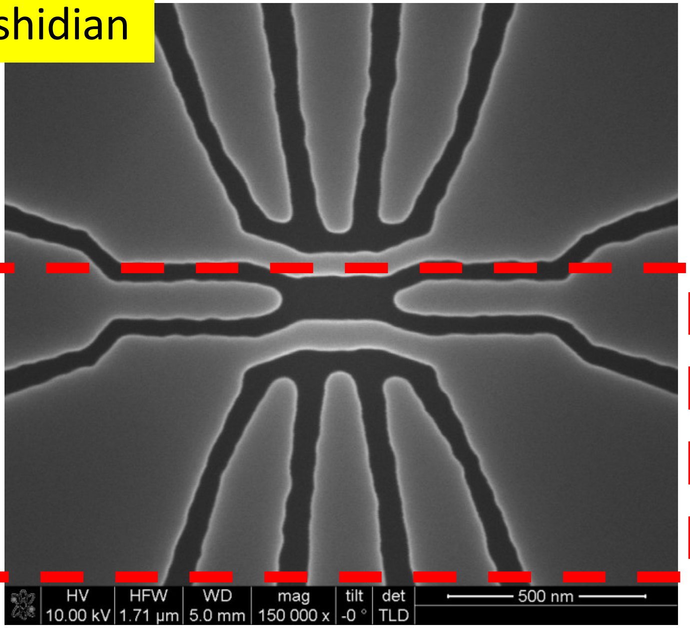

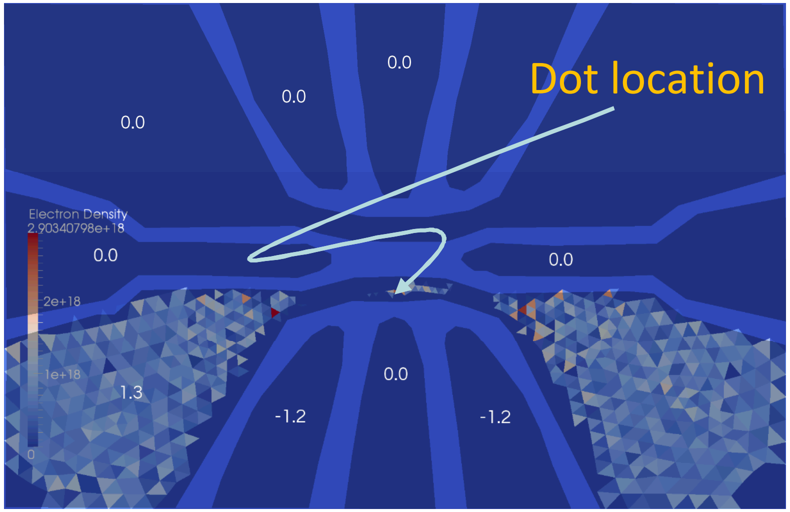

Metric	Measured (N=3)	Simulated (N=24)
Clp	2.2 +/- 0.3	2.3
Crp	2.1 +/- 0.4	2.1
Clc	3.7 +/- 0.3	4.1
Cl	2.1 +/- 0.2	2.4
Cr	2.0 +/- 0.2	2.0
Cag	17 +/- 1.3	26.2 (29, N=100)
Vth		

- QCAD is semiclassical simulation capability develo
- $1.1 \times 10^{17}/cm^3$ charge fits 4K threshold
  - Order of $\sim 5 \times 10^{10}/cm^2$
- Gate to quantum dot capacitances are similar to C multiple devices
  - Order of 20-30% disagreement in many cases

Tunable to few electron regime

Upper wire charge sensor

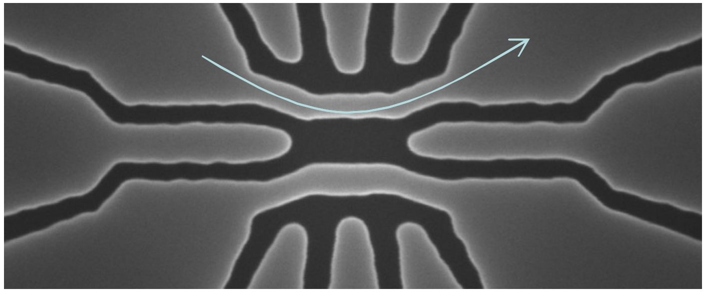

Charge sensed to last visible QD transition

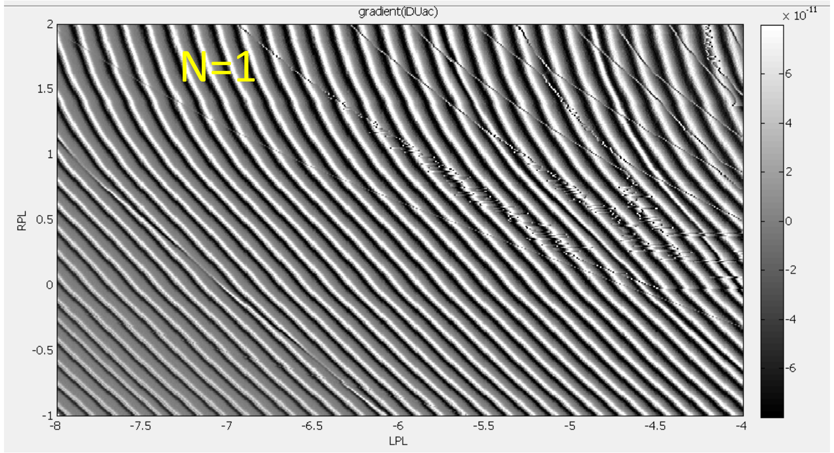

Bias configuration

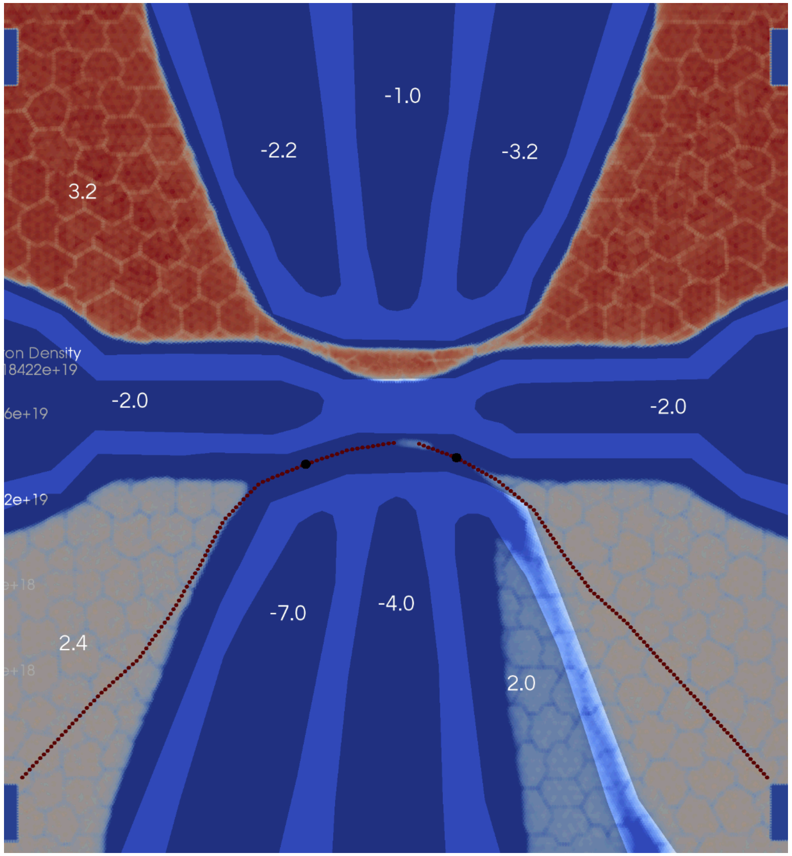

Dot shifted towards right lead to empty
Tunnel barriers continually opened to help verify

Opening tunnel barrier at few electron limit

CS current (derivative)

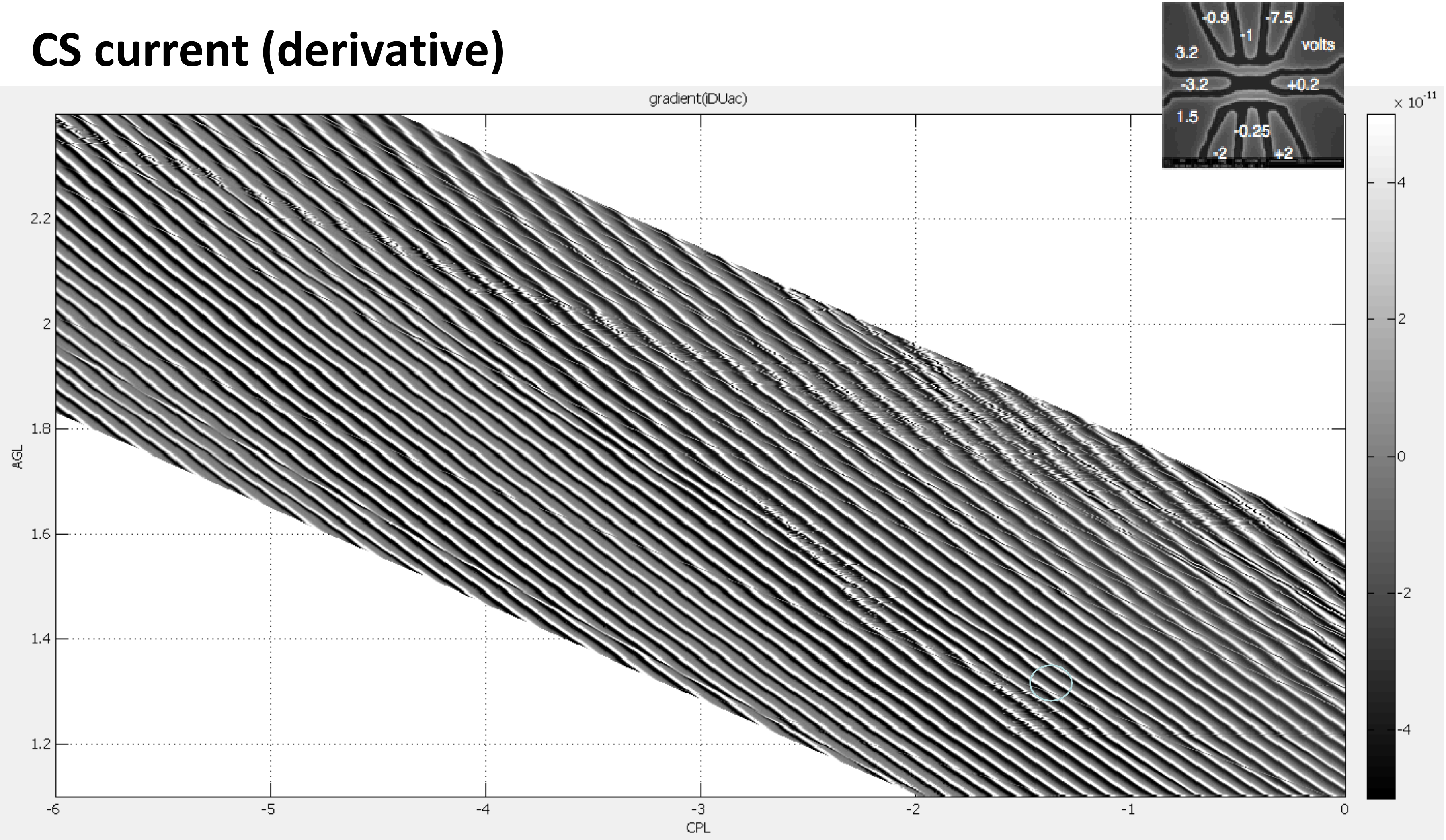

Gate wire with implant – QD coupling to donor

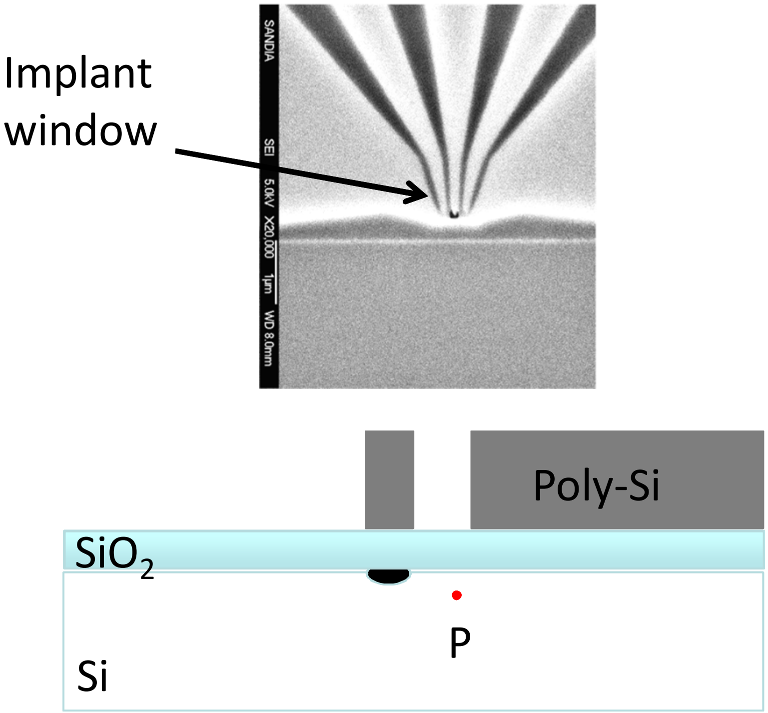

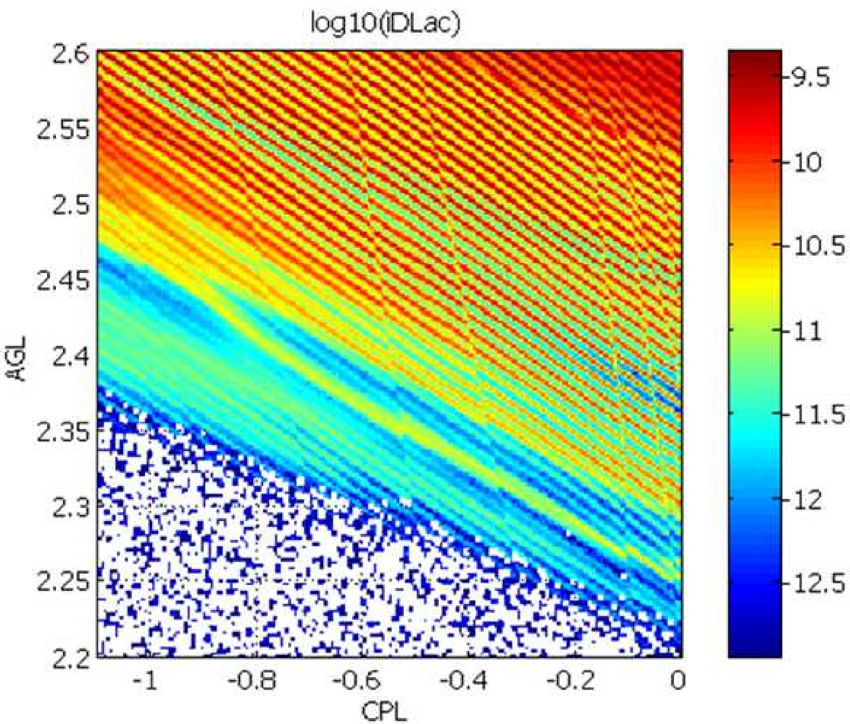

- Typical implant conditions:
- 45 keV implant, 8e11/cm^{-2} dose → ~ 50 P donors in window
- Charge offsets are seen in these implanted poly-MOS devices

Tuning spin readout

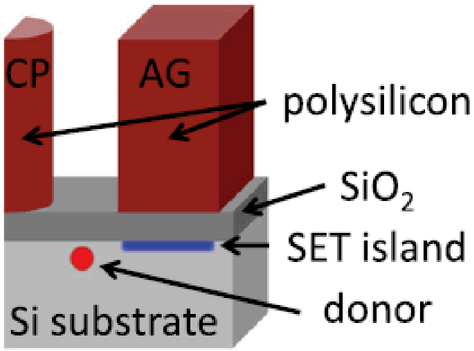

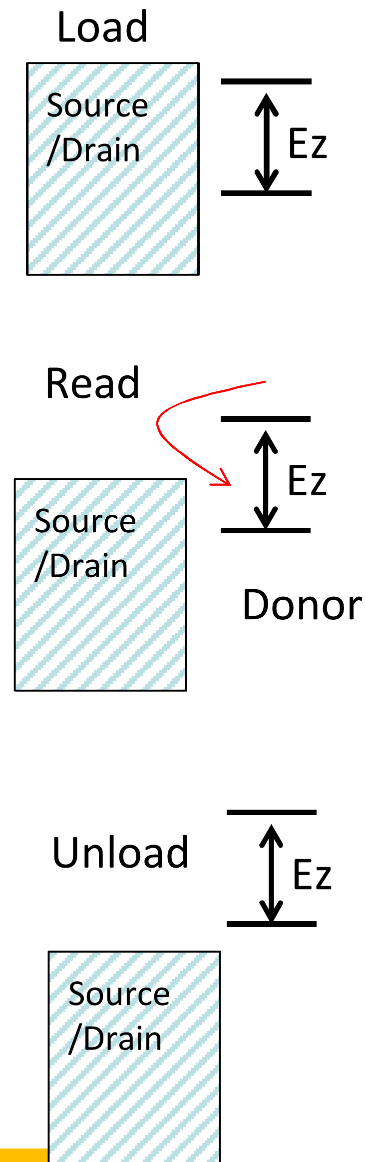

Spin bump with 256 averages

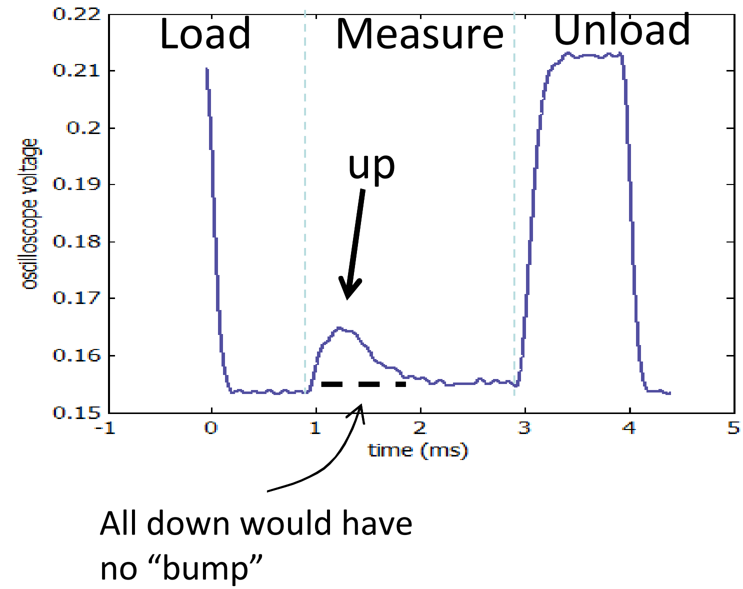

- T1 observed to have B^5 dependence
- Wilson & Feher ensemble Sb: T_1 = 1111 s at 1.25 K, B = 0.8 T for B along (100) direction
- Fairly close when kT scaled (T_e~400 mK)

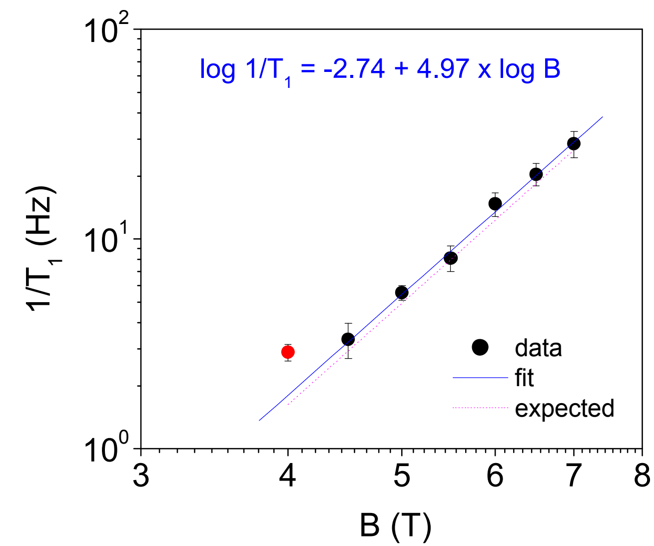

Tracy et al. APL 2013 (Sb donor)

Tuning spin readout

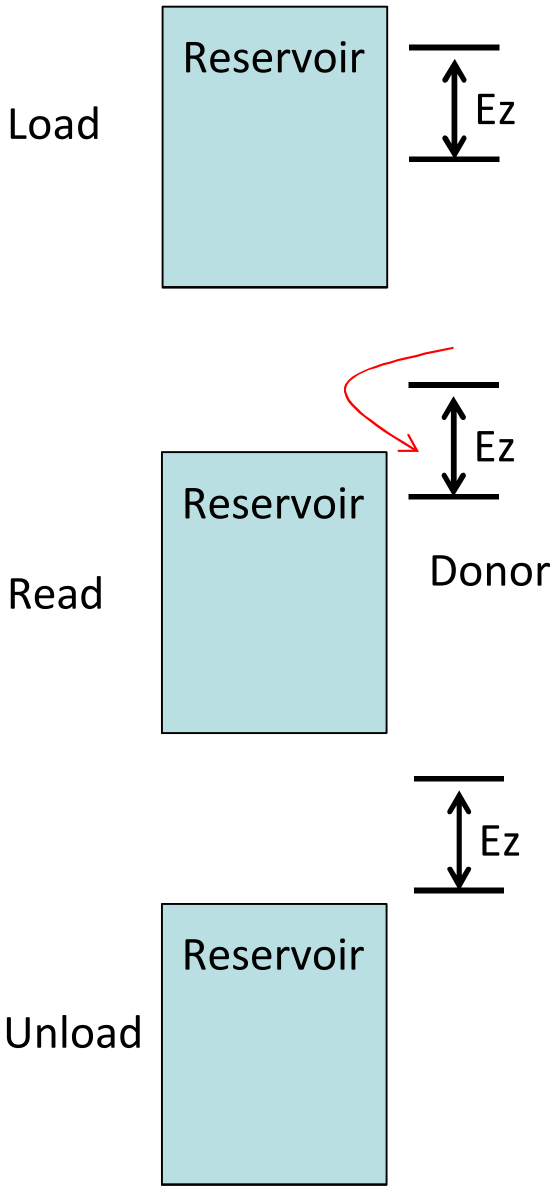

Spin bump with 256 averages

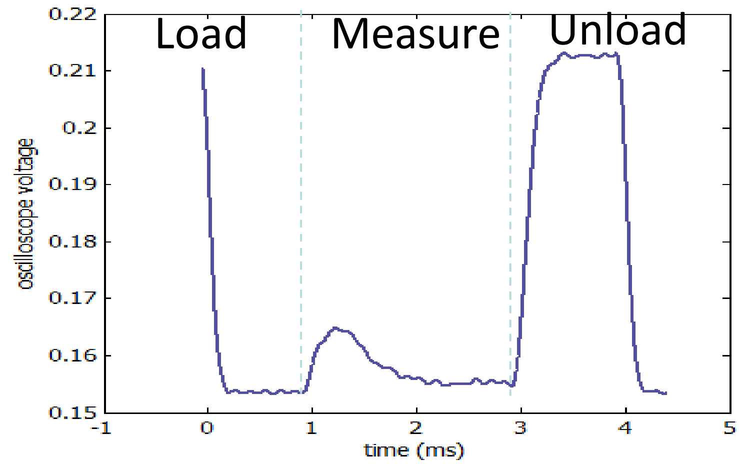

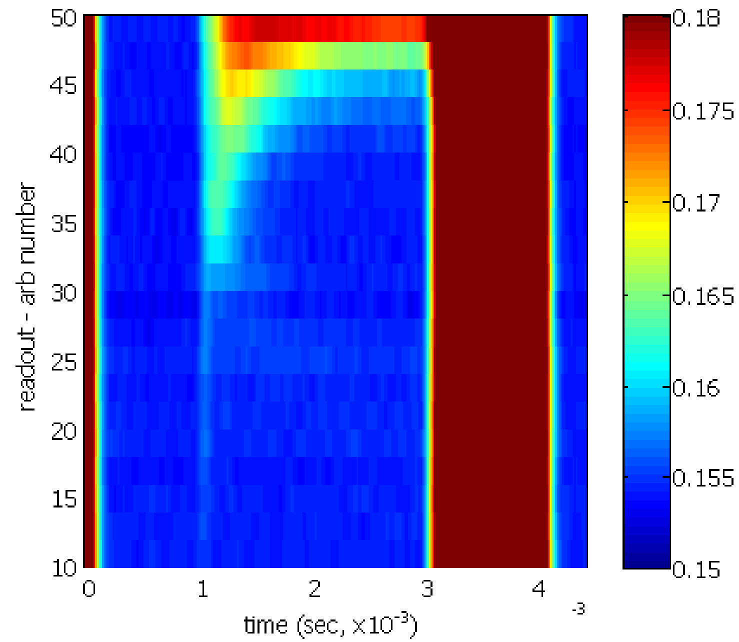

Motivation for HBT

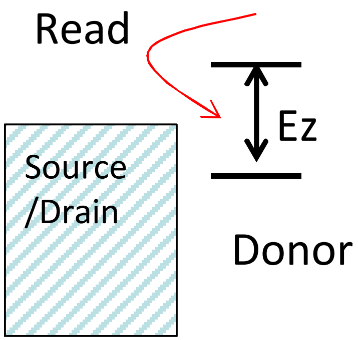

- Goal: Extended circuit bandwidth for fidelity and increased time resolution.
- Challenge:
  - for donor spin read-out RF-SET/QPC introduce varying S/D voltage
  - Additional cost/infrastructure and effort for RF-SET/QPC

One option: HEMT (High Electron Mobility Transistor)

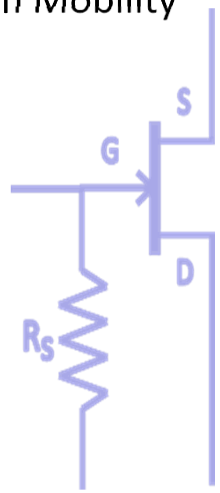

- Field Effect Transistor (FET).
- Shunting resistor Rs for voltage input.
- DC power dissipation of 10 μW to 1 mW.

An alternative: HBT (Heterojunction Bipolar Transistor)

- Bipolar Junction Transistor (BJT)
- Current input into the base.
- We chose a commercial HBT model based on measured performance at low temperature.
- No shunting resistor -> no (Rs*C) time constant.
- We measured a DC power dissipation of 50 nW to 10 uW.

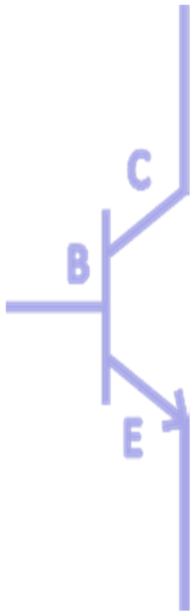

HBT performance

Matt Curry (U. New Mexico)

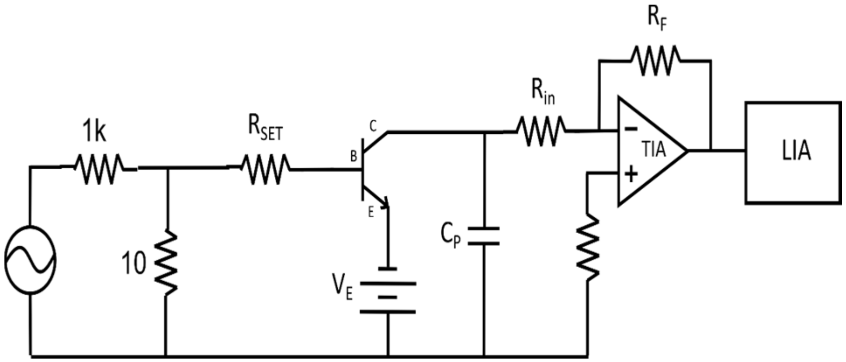

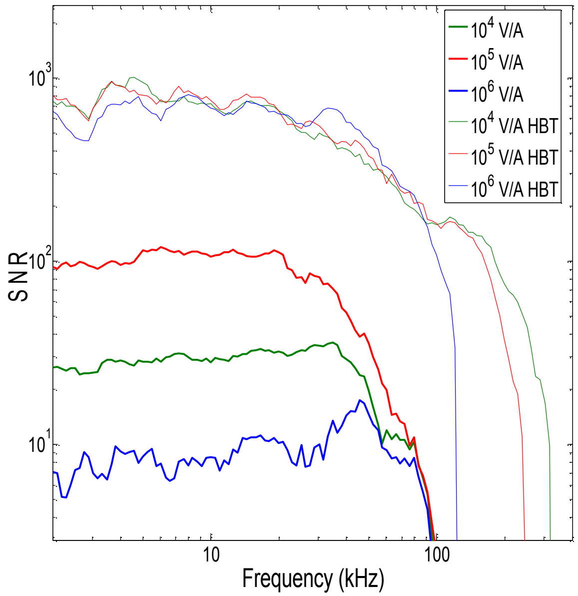

- Bandwidth is extended using HBT
- S/N appears to be improved
- HBT response is non-linear

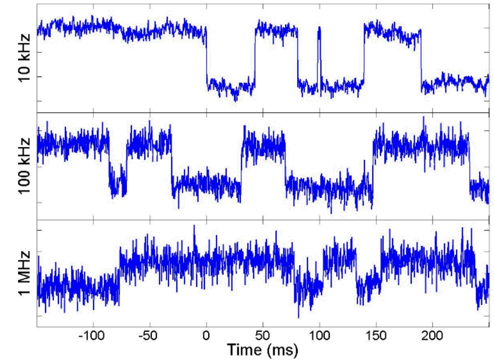

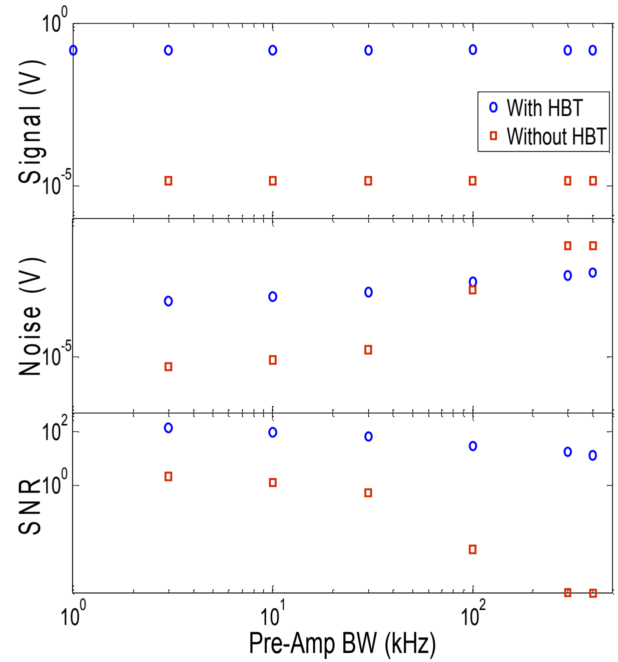

Pulsing On Source With HBT
Compared to Without HBT (Calculated)

ESR pulse sequence – two level pulse

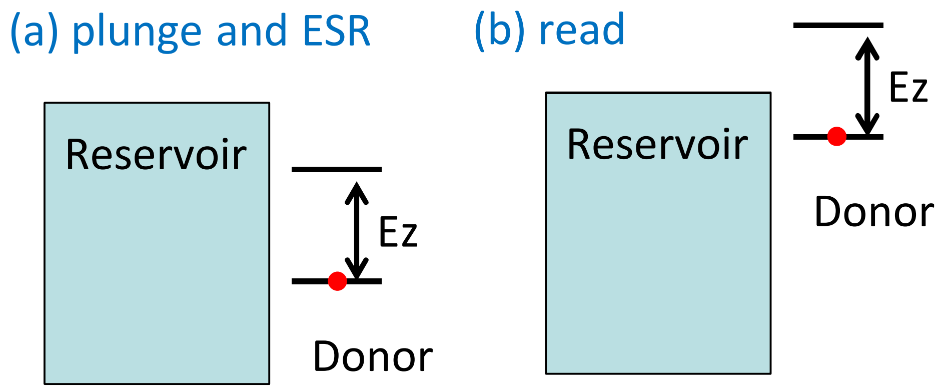

1. At the end of the readout pulse, a spin down is loaded. (b)
2. Pulse energy levels down to manipulate. (a)
3. Apply microwaves. (a)
4. Spin readout (b)

ESR pulse sequence – two level pulse

(a) plunge and ESR

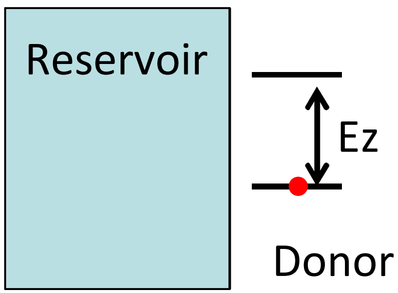

(b) read

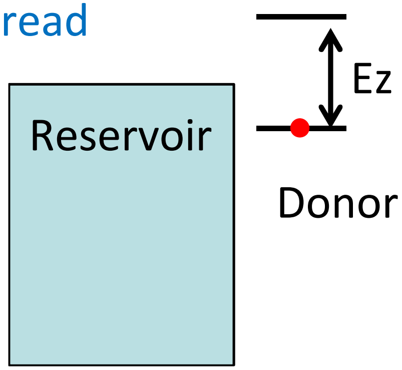

1. At the end of the readout pulse, a spin down is loaded. (b)
2. Pulse energy levels down to manipulate. (a)
3. Apply microwaves. (a)
4. Spin readout (b)

Off resonance – no spin up signal

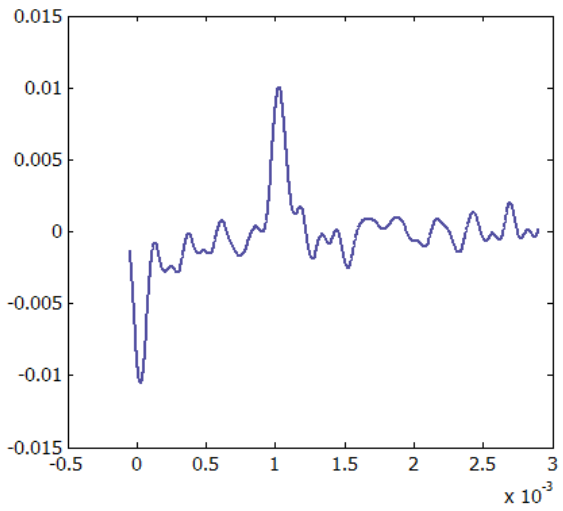

Electron spin resonance of single spin

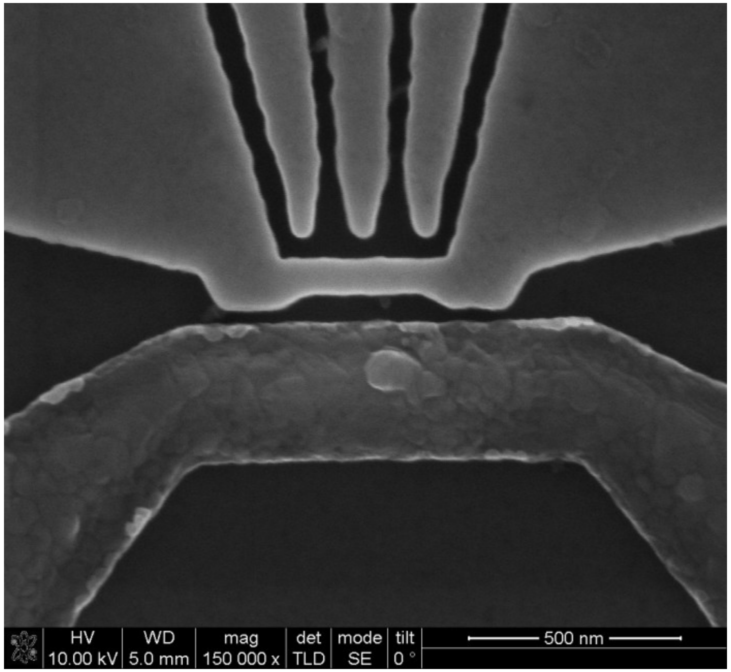

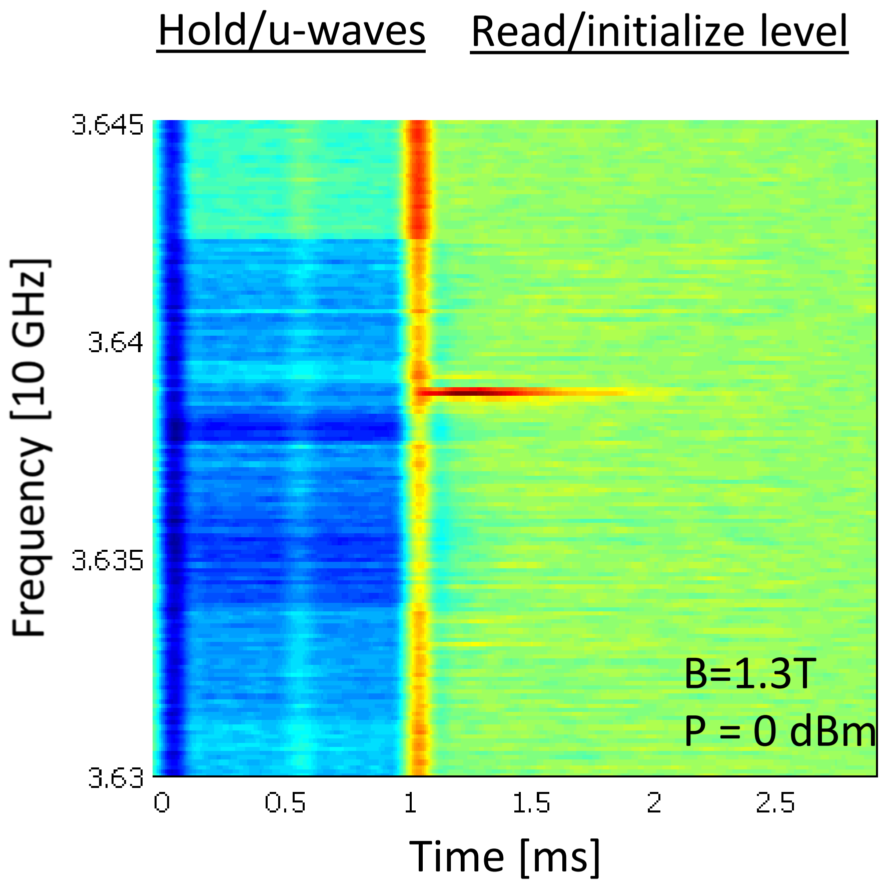

- Two level test with ESR detects spin resonance
- Phosphorus implanted sample (~ 400 nm from center)
- Similar approach to Al-Si SET devices [Pla et al. (2012)]

Nguyen

Sandia National Laboratories

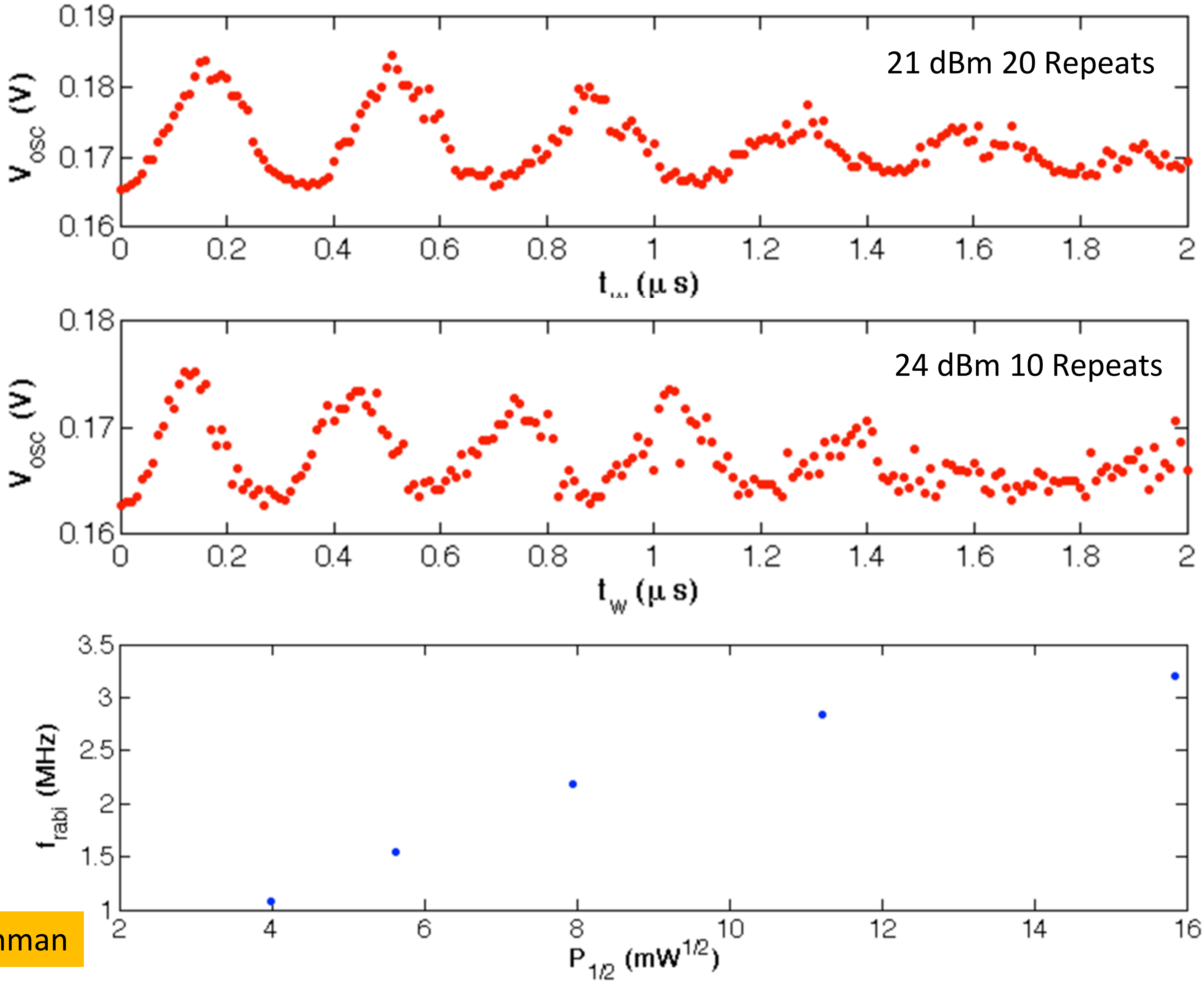

21 dBm 20 Repeats
24 dBm 10 Repeats
V_{osc} (V)
t_w (μ s)
f_{rabi} (MHz)
$P_{1/2}$ ($mW^{1/2}$)

Luhman

Resonance frequency drifts

These two scans were taken 10 min apart.

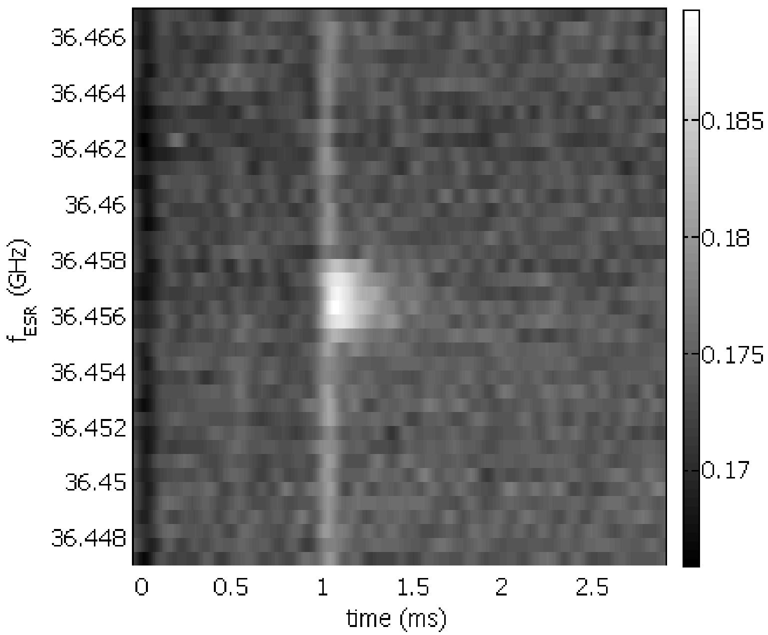

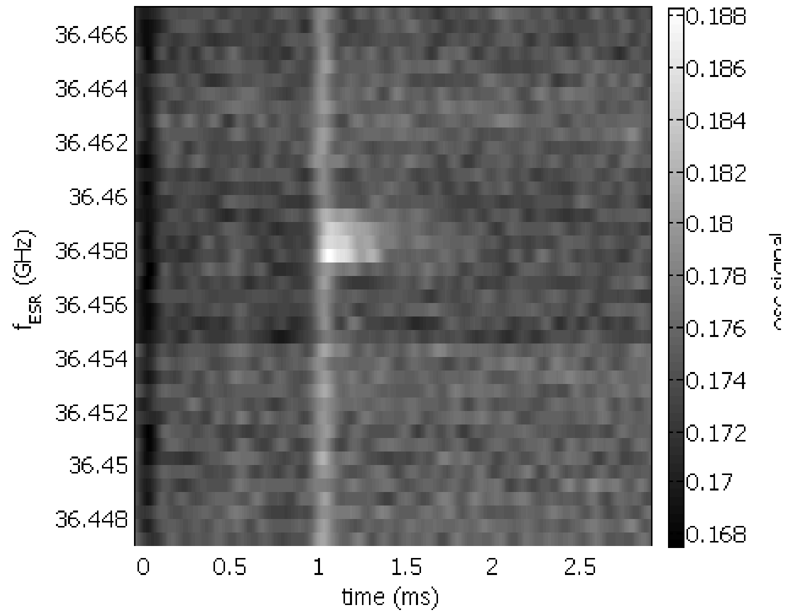

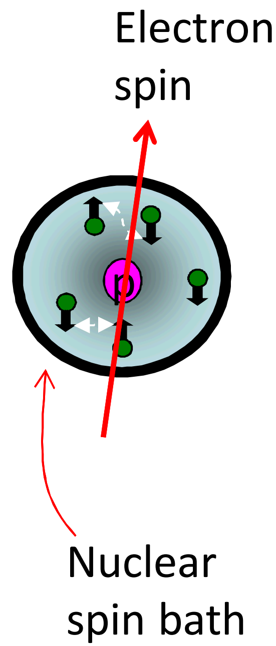

- ^{29}Si can reorient over timescales of ~sec, and the electron resonance frequency shifts due to hyperfine coupling.
- ~5-10 MHz line width or equivalent of ~ 0.2-0.3 mT
- B_{ac} max ~0.1 mT

Adiabatic inversion (pi rotation)

Rotating frame

$$\widetilde{H}_Q = \hbar\Delta\omega\sigma_e^z + \mu_B B_{ac}\sigma_e^x$$

$$\mathbf{n} = \hbar\Delta\omega\hat{k} + \mu_B B_{ac}\hat{i}$$

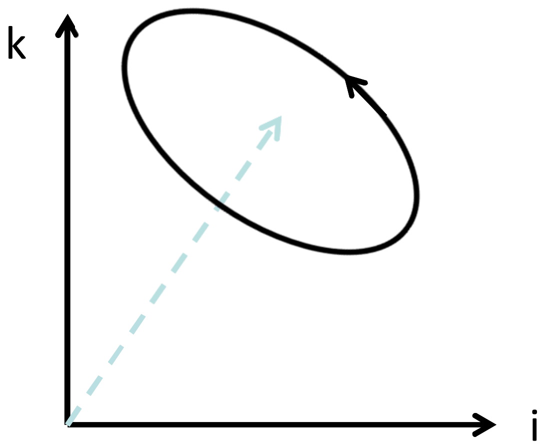

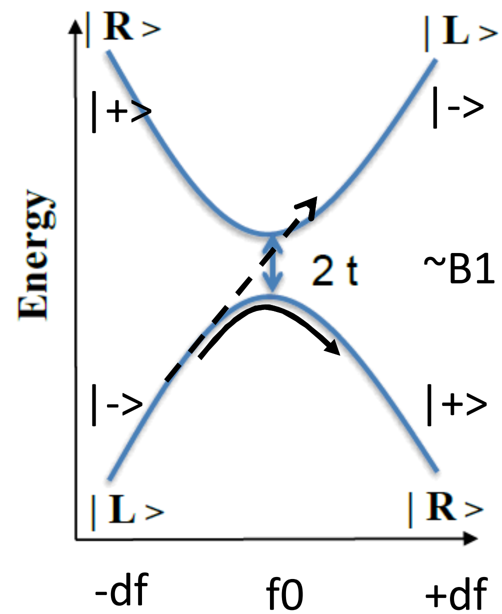

- Magnetization follows a complicated track in lab frame
- Constant precession around Z-axis can be separated out in rotating frame
- ESR pulse for X rotation is notionally a diabatic pulse when on resonance
- Adiabatic inversion starts off resonantly and transitions slowly through resonance

Adiabatic sweep compared to on-resonant pulse

Electron spin

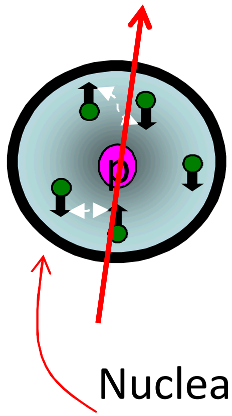

Nuclear spin bath

Pulsed pi rotation “on resonance”

Spin bump signal

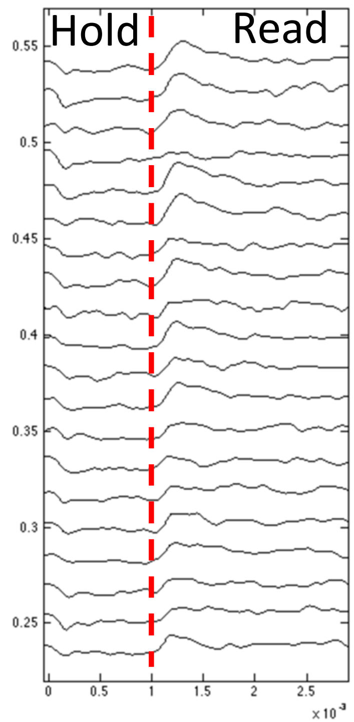

Adiabatic Sweep

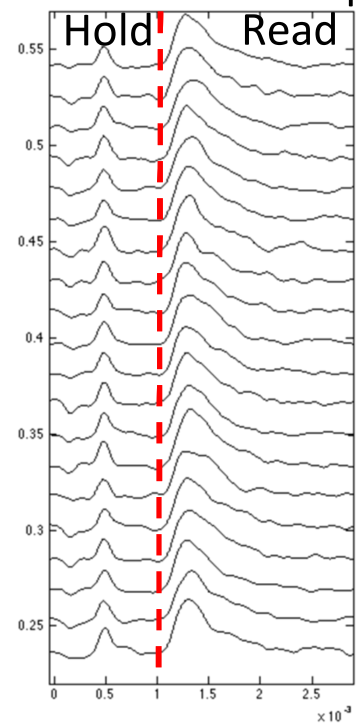

Adiabatic approach

$$P_{up} \propto 1 - e^{-\frac{\pi^2 f_r^2}{\Delta\nu / t_{pulse}}}$$

$\Delta f/t << f_{rabi}^2$

$\Delta f = 25$ MHz; $t = 10$ us

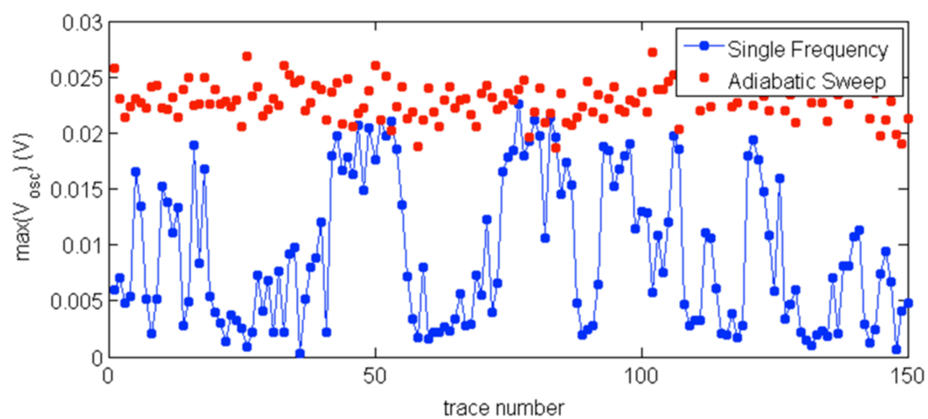

Luhman

Characterization of adiabaticity of sweep

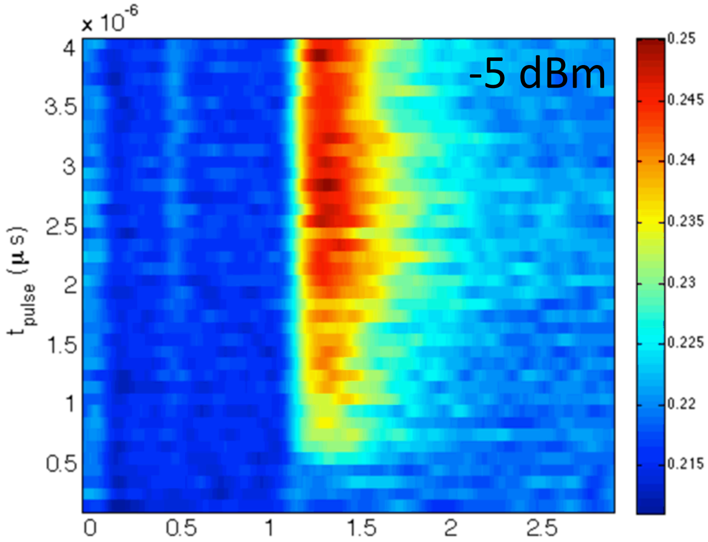

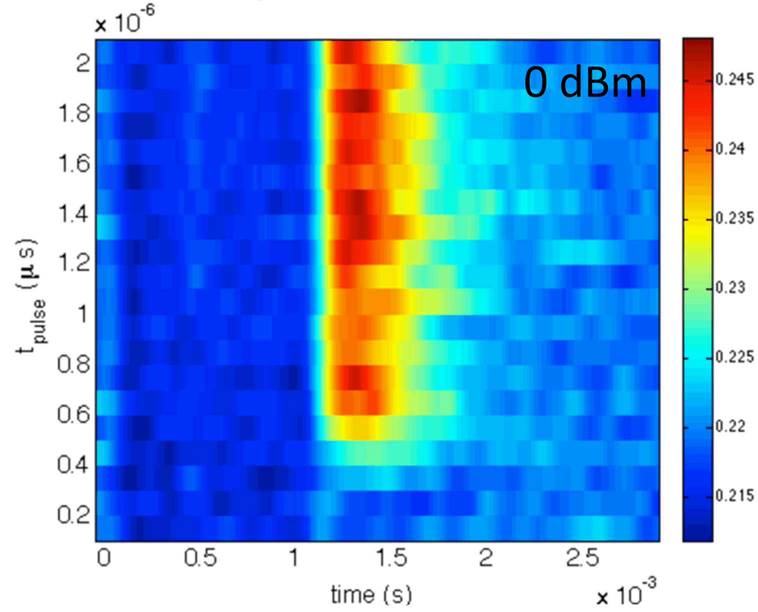

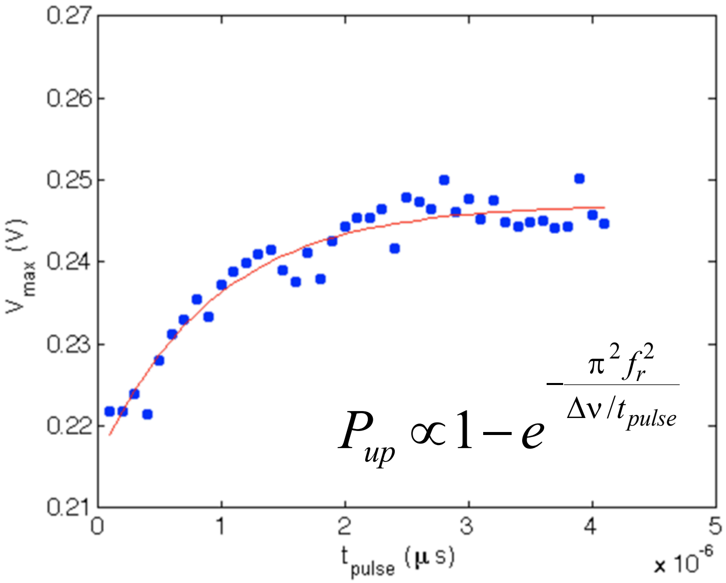

$$P_{up} \propto 1 - e^{-\frac{\pi^2 f_r^2}{\Delta\nu / t_{pulse}}}$$

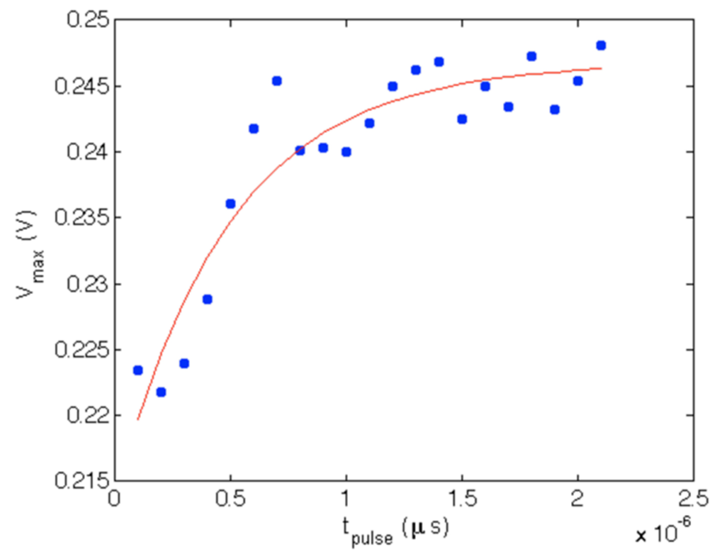

Luhman

Rabi Oscillations with BIR4-WURST

Data taken in a very similar (but slightly different) way as "normal" Rabi oscillations

- ESR power: 15 dBm
- 2048 averages
- Measured θ from 0 to 8π in steps of $\pi/10$
- Blue line is a fit to the equation: $a*\sin(\theta/2)^2+c$

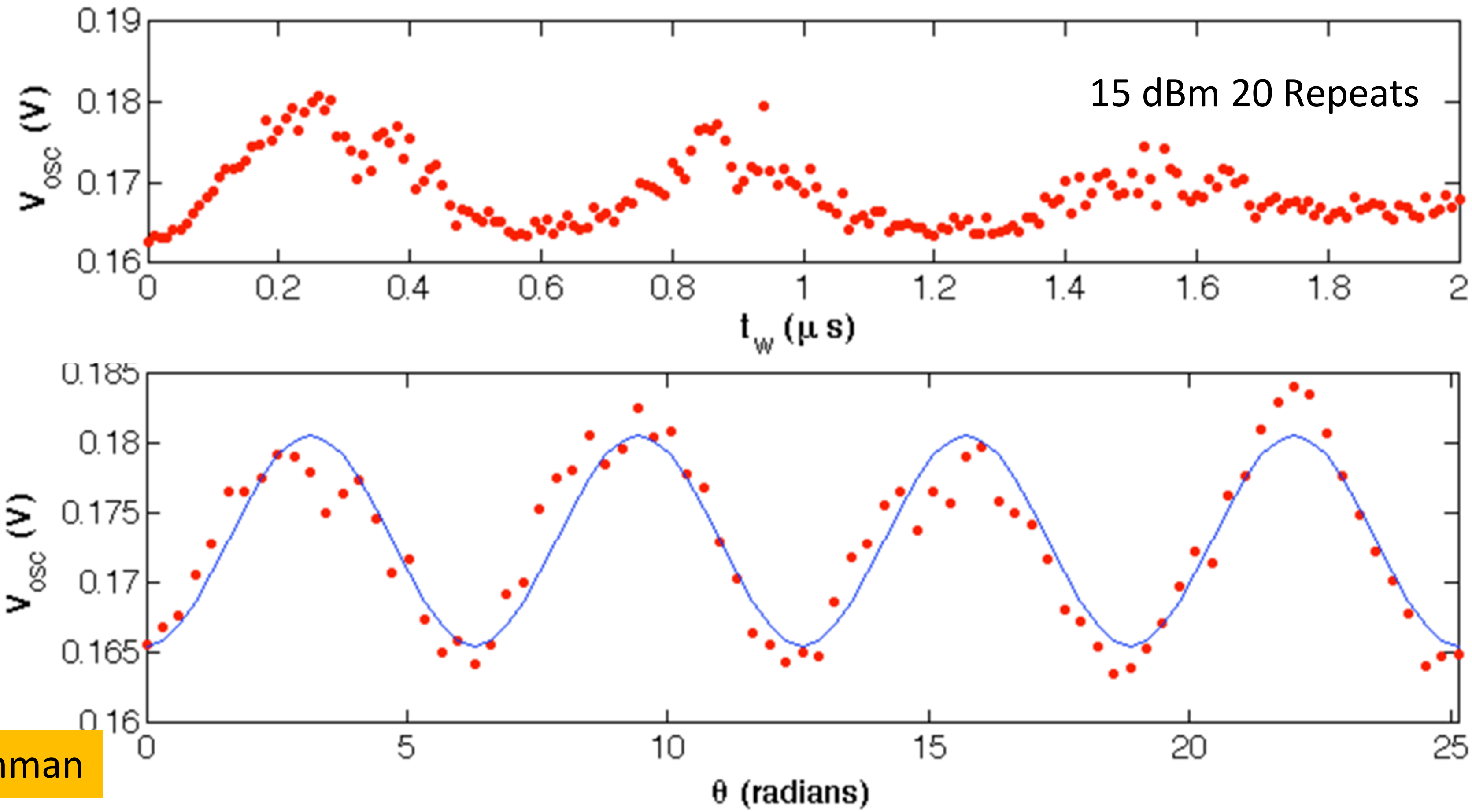

Luhman

Single spin spectrum

WURST pulse

Run	Offset	Step
1	1 MHz	0.5 MHz
2	1 MHz	0.5 MHz
3	0.5 MHz	0.25 MHz
4	0.5 MHz	0.25 MHz
5	0.5 MHz	0.25 MHz

104 MHz in range of previous single P reports
5 MHz splitting could be 29Si
Uncertainty in identification related to centered lines

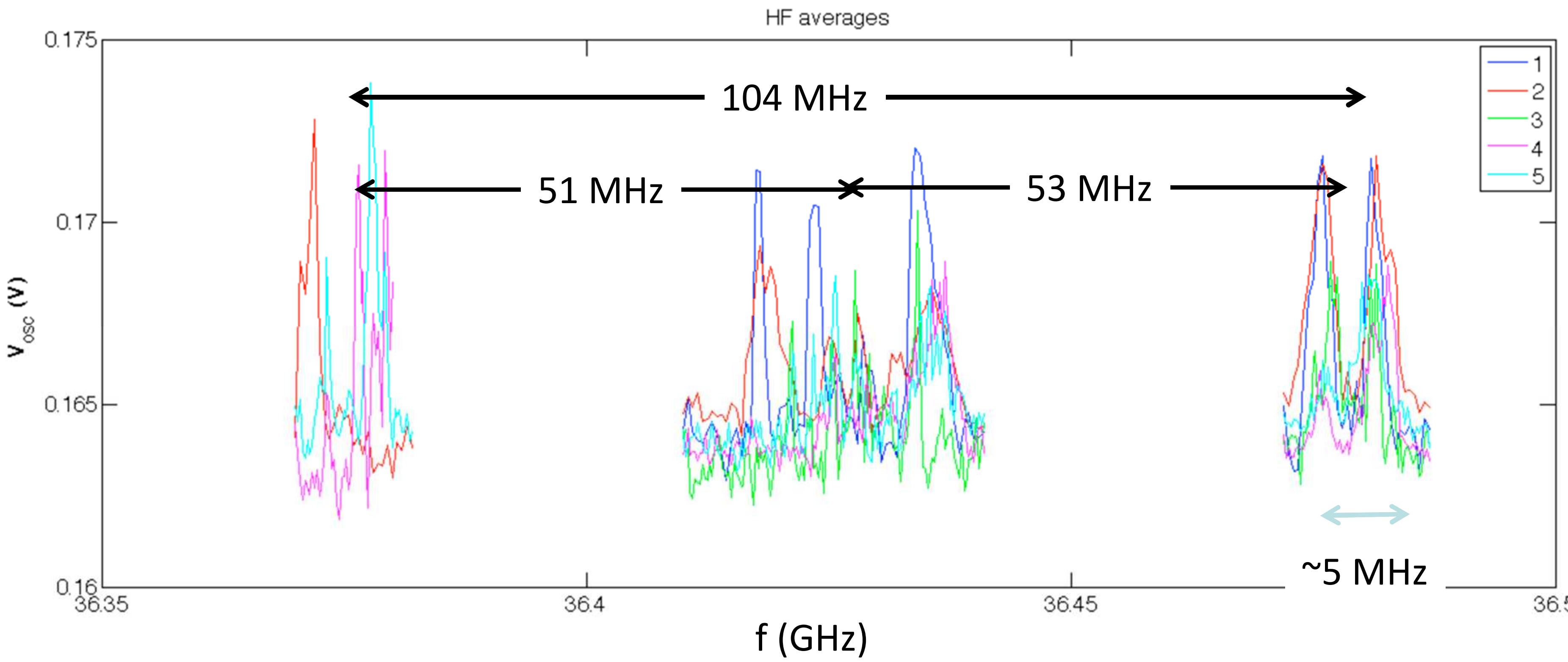

Outline

- Motivations
- MOS donor qubits
- Two qubit nanostructures
  - Single ion implant
  - SiGe/sSi STM
- Summary

Donor-donor coupling concept

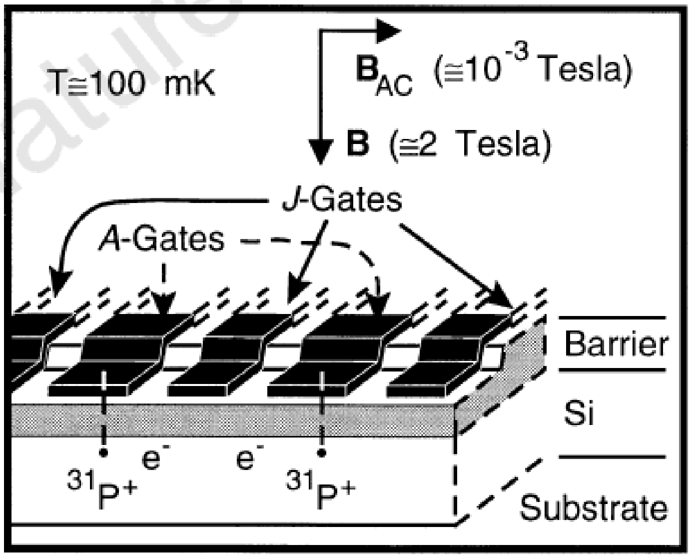

Kane (1998)

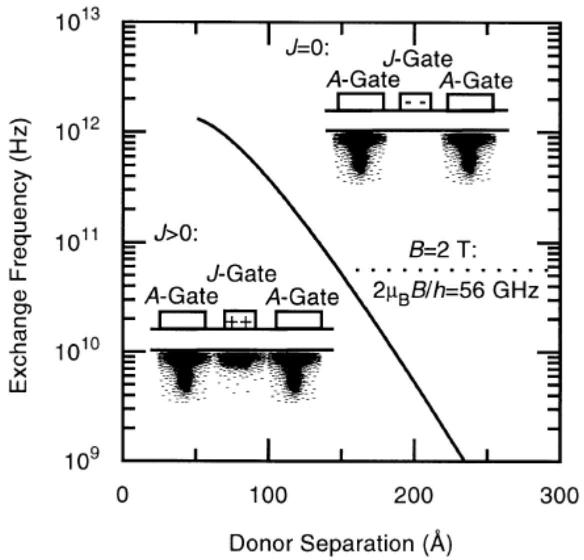

- Vision: Kane-like architecture with exchange gate
- Can this really be done?
- Can it be done with this configuration?

J dependence on depth & spacing (no J-gate)

Low vertical E-field

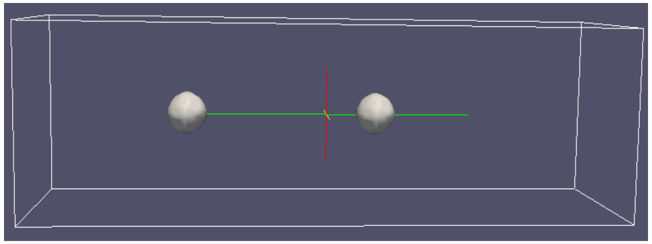

High vertical E-field

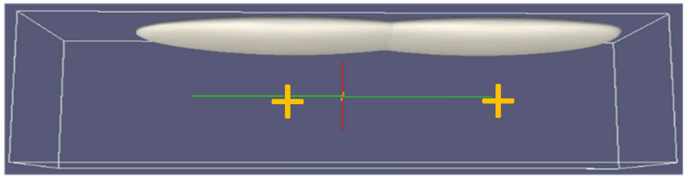

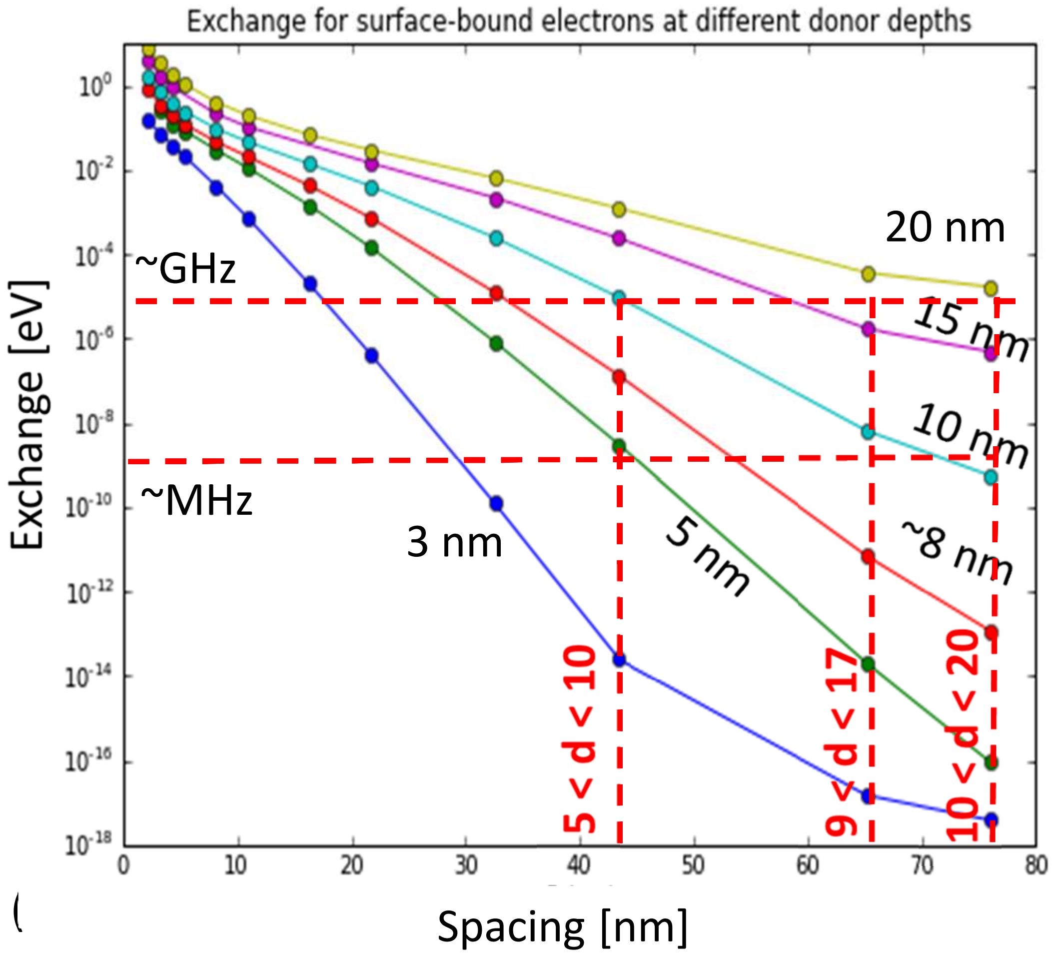

- EMT calculations from Calderon et al. addressing J after ionization (JAP 2009)
- Target gate speeds order GHz to MHz
- If you choose target spacing 70 nm +/- 5 (each donor)
    - Target depth: 13.5 nm +/- ~3.5
    - Introduction of J-gate between relaxes the spacing requirements but d < 15 nm for rapid adiabatic passage to surface

NEMO calculations: Muller et al.

Getting to single donors w/ the CMOS approach

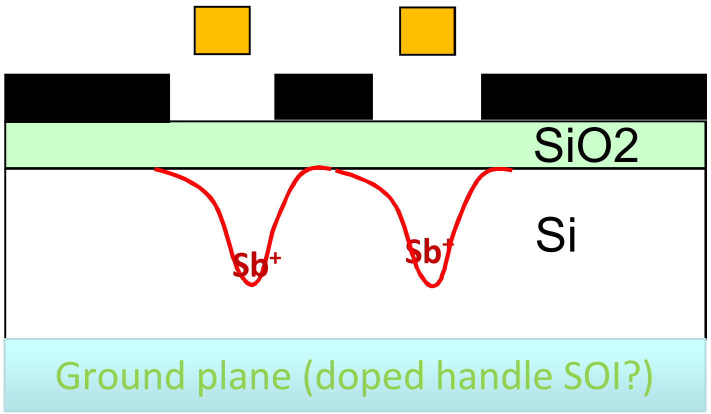

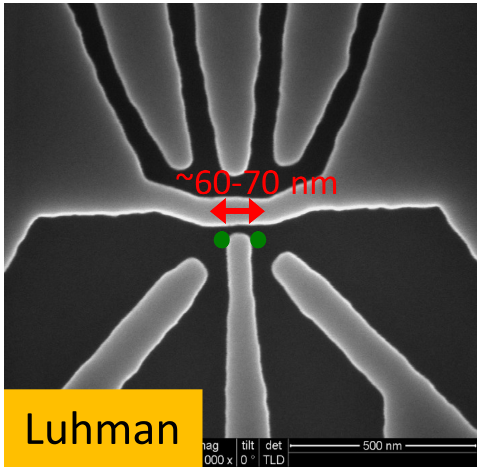

- Approach
  - Integrated diode detector senses arrival of single ion
  - E-beam lithography or advanced litho (EUV) defines lateral position
  - Energy of ion determines vertical position

Adiabatic wavefunction shift to surface

Calderon et al., PRL 2006

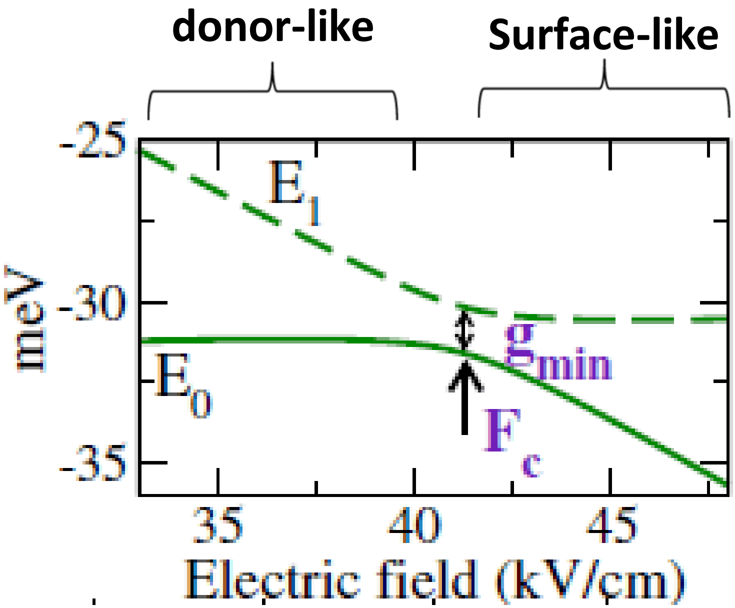

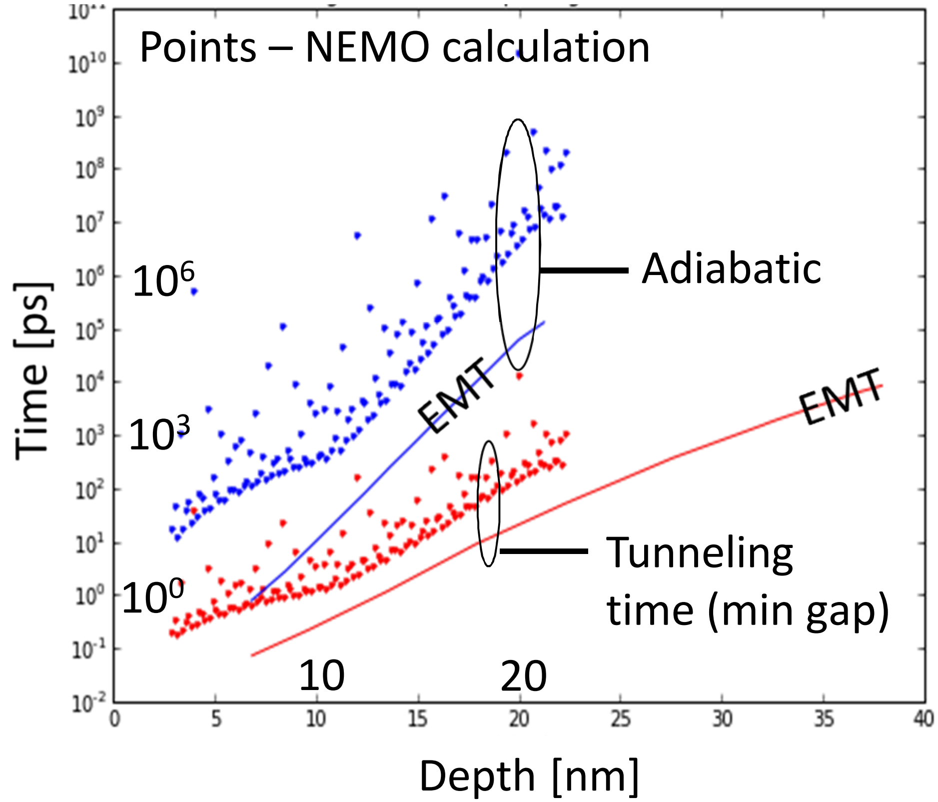

- Adiabatic transfer for systematic phase
- Transfer times must be fast relative to J
- Overall conclusion: adiabatic transit times are sufficiently fast for donors D < 15 nm
- Fine print: tilt impacts values because of effect on valley splitting at surface
- 10 keV < E < 55 keV (Sb)

Ion	Energy (keV)	Range (nm)	# e-h pair
P	24	36 ± 16 ± 13	~2500
Sb	55	36 ± 10 ± 8	~4600
Sb	10	12 ± 3 ± 3	~600

Approach: devices fabricated w/ single ion detection

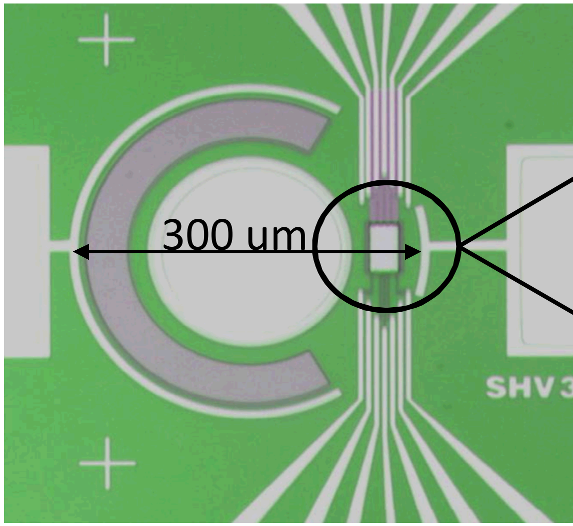

Ion Beam Induced Charge (IBIC) map

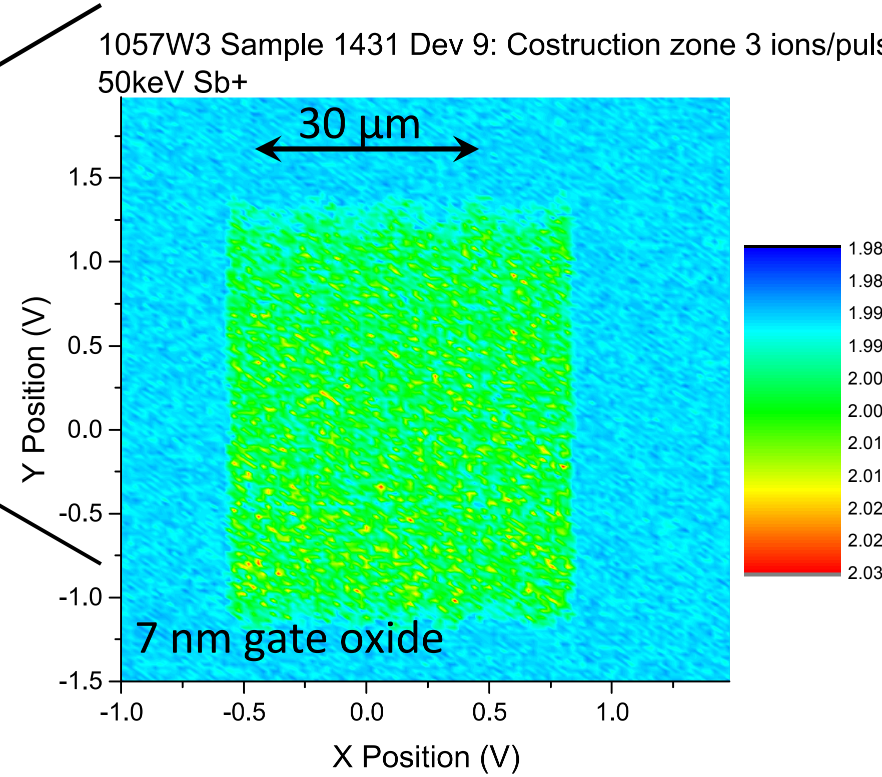

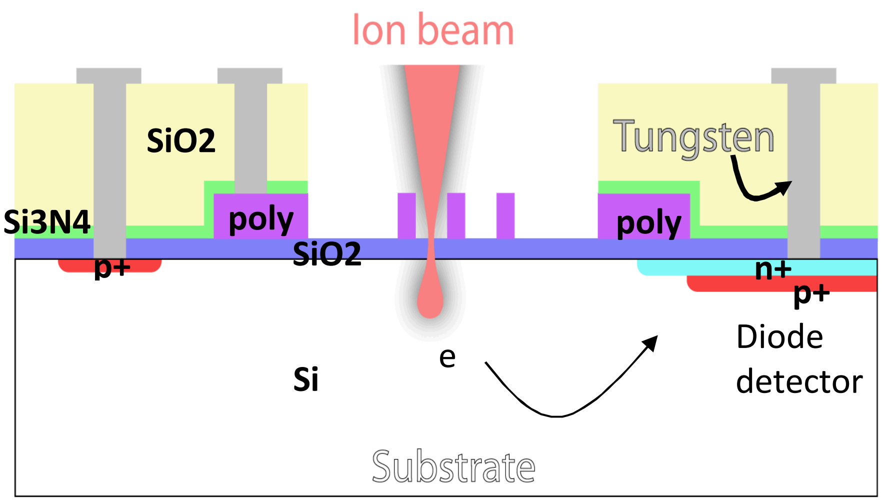

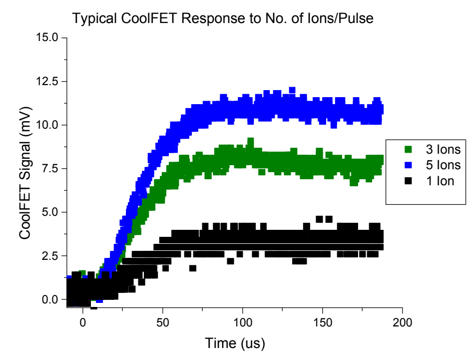

Good S/N at <N>=1

Geiger mode also working now

Effect of donor on transport - offsets

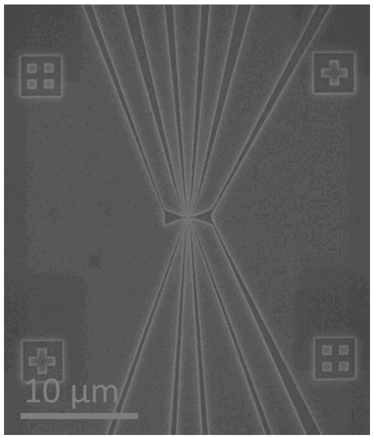

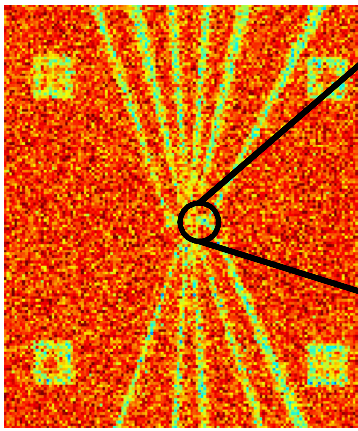

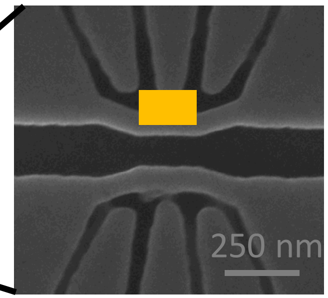

50 keV Sb+
~ 20 donors in
window of interest

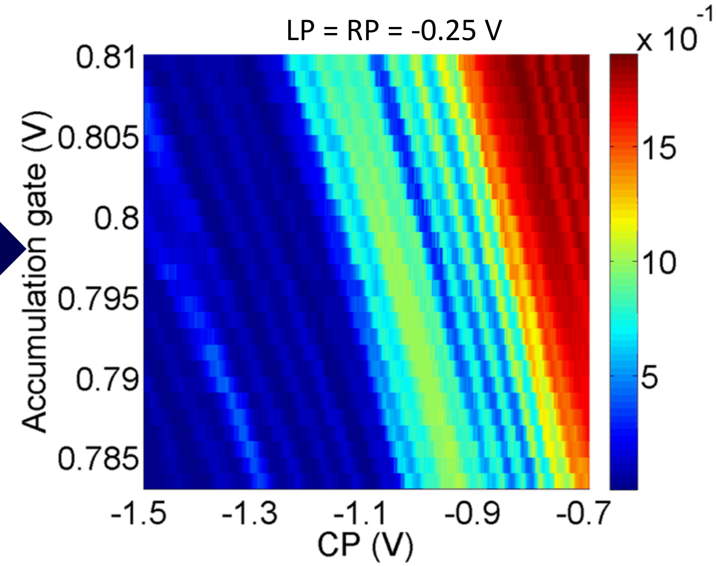

http://www.toonpool.com/cartoons/

Why can we not see donors in transport?

1. Systematic differences in 7 nm vs. 35 nm device
2. Other possibilities

Donor-QD two spin system

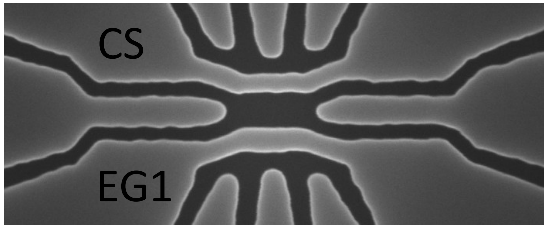

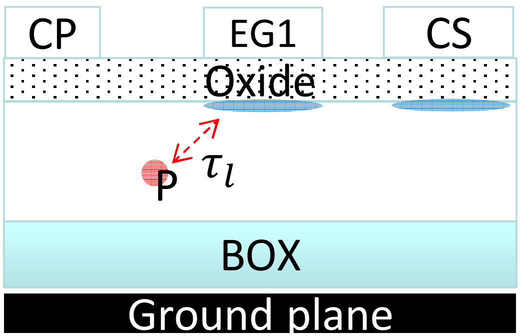

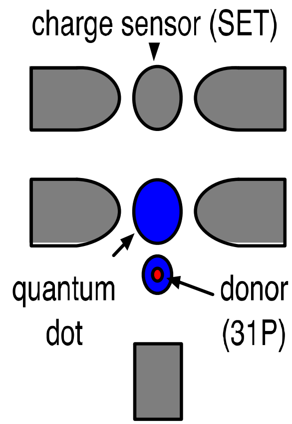

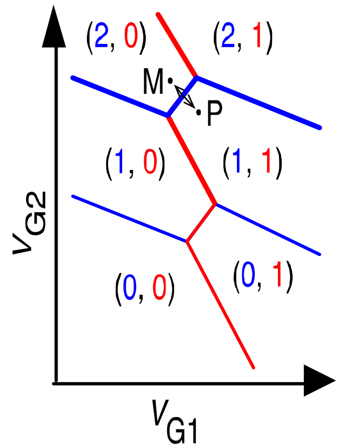

Petta et al. Science 2005

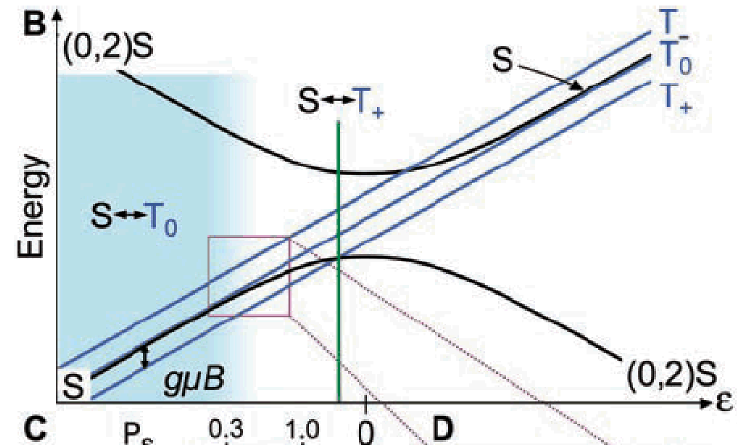

- Charge sensed donor-QD system is experimental platform:
  - Look at transfer to surface
  - Look at two spin exchange (w/ QD spin)
  - Donors on both sides for D-D exchange mediated by dot

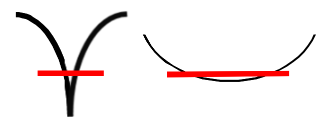

$$H = \begin{pmatrix} J(\varepsilon) & A(V) \\ A(V) & 0 \end{pmatrix}$$

QD-D anti-crossings

Looking for Spin blockade QD-D anti-crossing

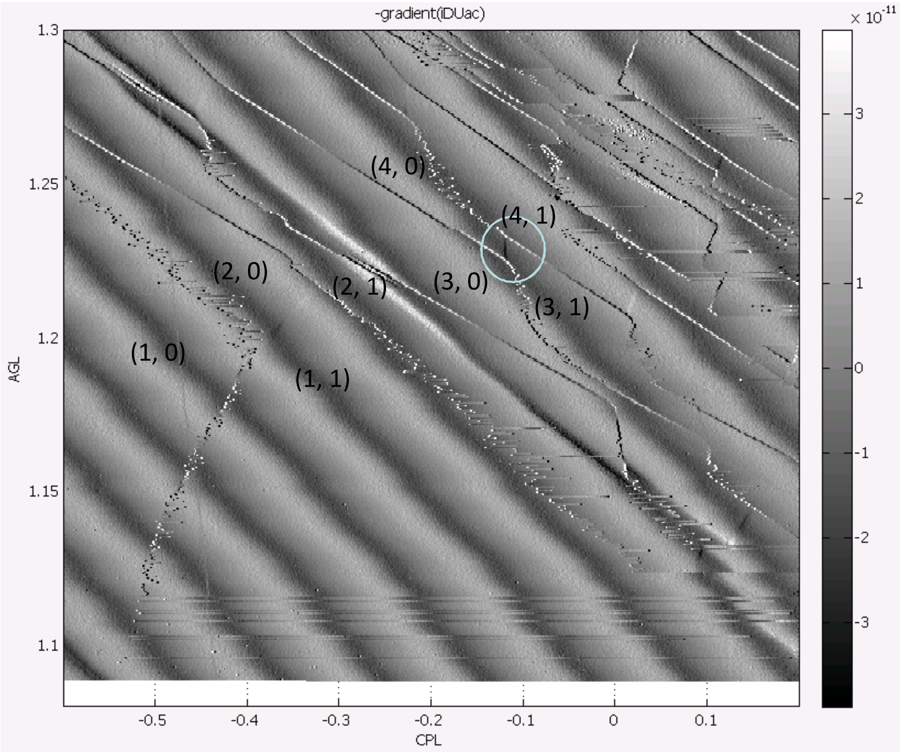

(4,0) <-> (3,1) transition

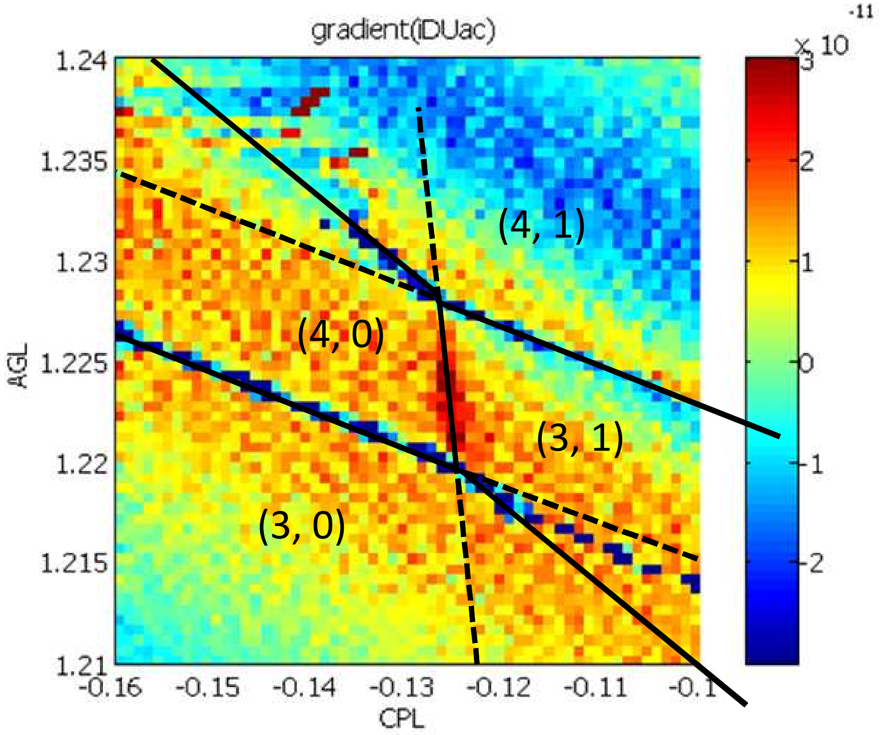

Two donor interaction

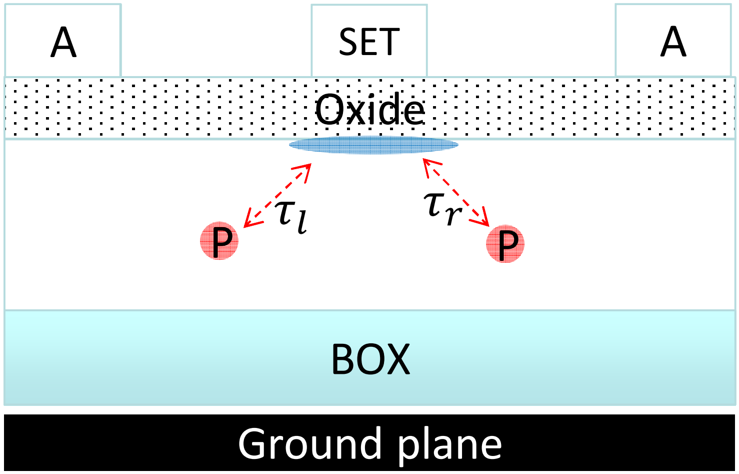

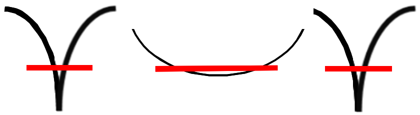

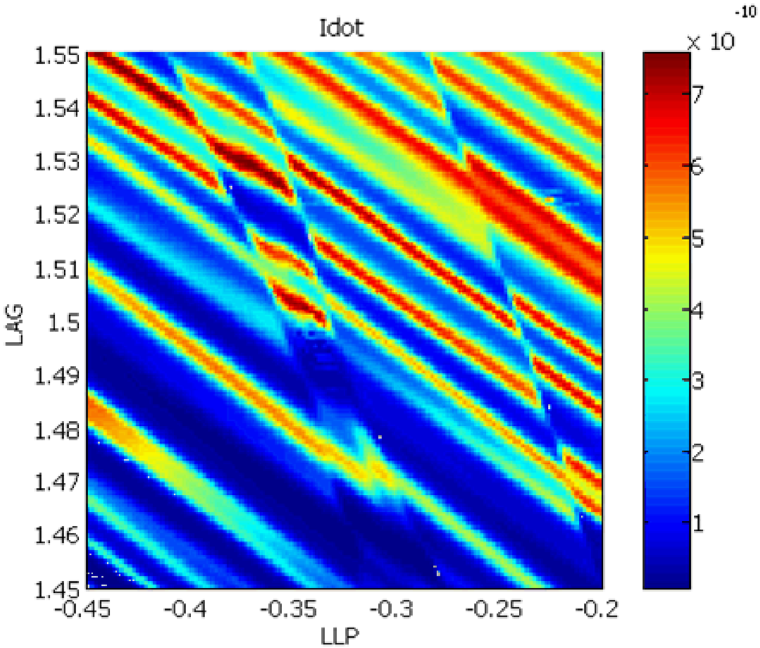

Outline

- Motivations
- MOS donor qubits
- Two qubit nanostructures
  - Single ion implant
  - STM
- Summary

Donor-donor coupling concept

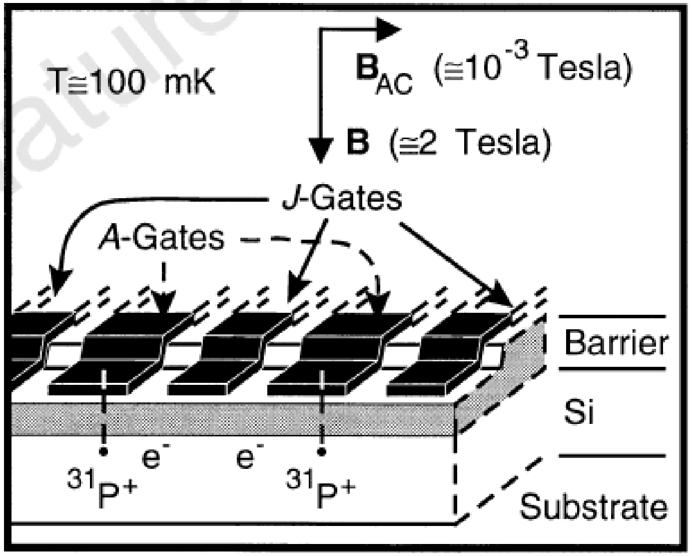

Kane (1998)

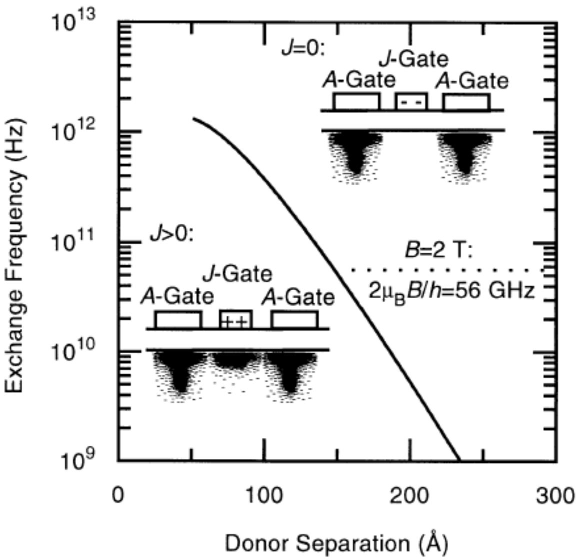

- Vision: Kane-like architecture with exchange gate
- Can this really be done?
- Can it be done with this configuration?

Ultimate lateral and vertical control of donors

1. Start w clean Si(001)

2. Adsorb H resist
Self-limiting 1 monolayer

3. Pattern w STM
Atomic-precision

4. Adsorb PH_3

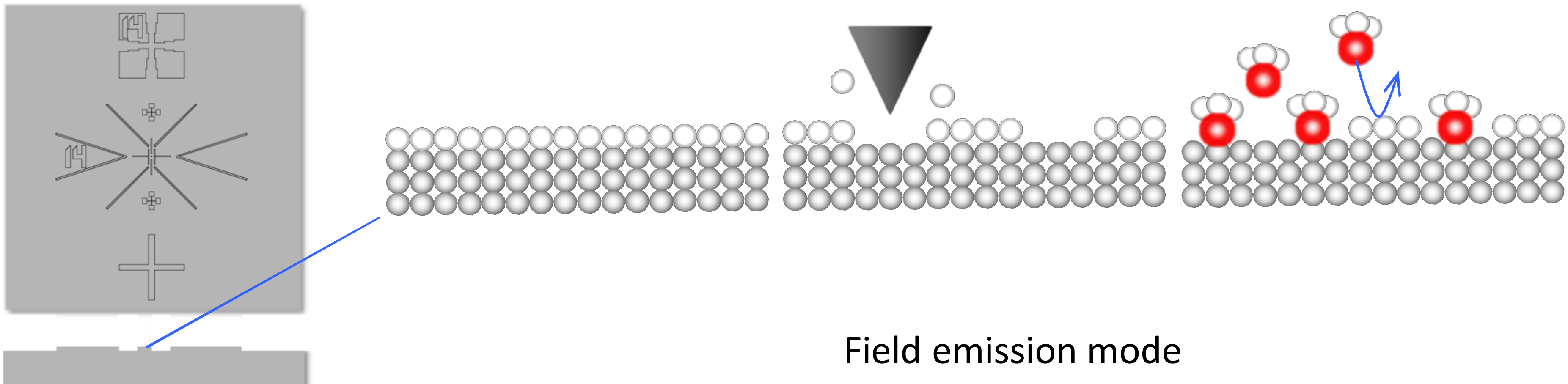

Etched alignment marks

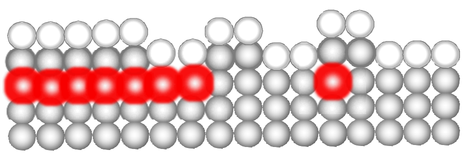

5. Incorporate P
-Anneal→ Si-P swap
-H resist constrains P

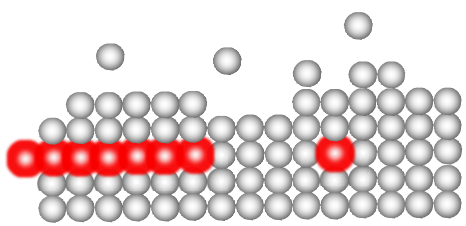

6. Desorb H & bury P in Si

Field emission mode tunnel barrier

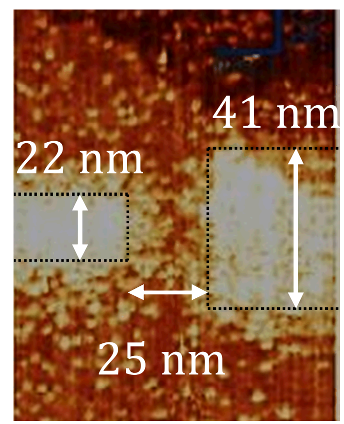

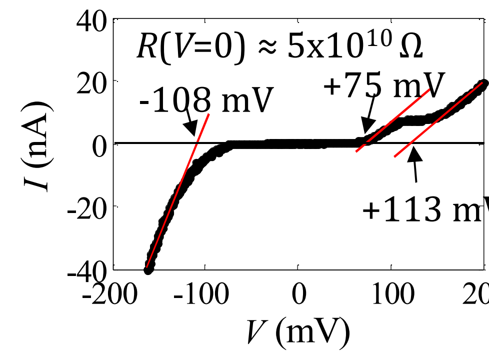

Bussmann & Rudolph

Field emission H-desorption mode

Typical tunneling mode

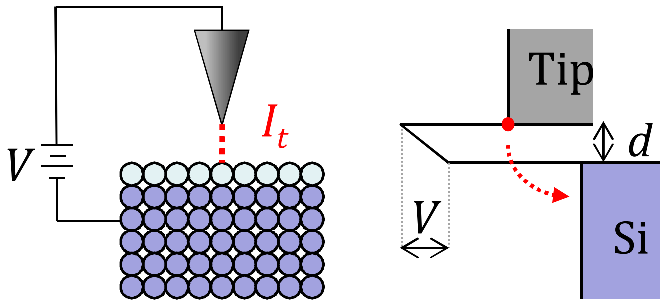

- $d \approx 1$ nm
- $V \approx 4$ V
- $I_t \approx 1$ nA
- Single atom spot size
- Scan rate ≈ 50 nm/s

Field emission mode

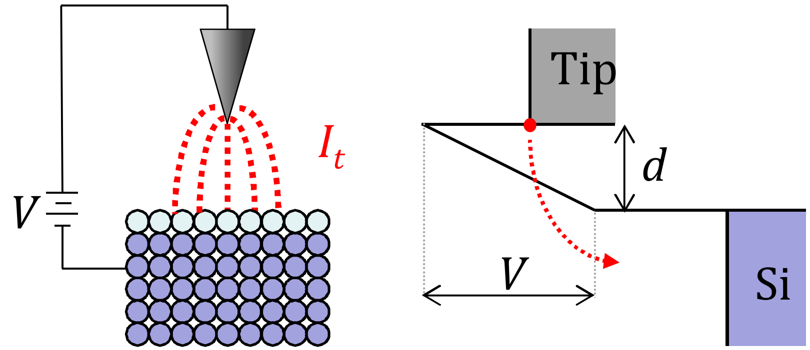

- $d > 10$ nm
- $V > 10$ V
- $I_t \approx 1$ nA
- Tunable spot size
- Scan rate ≈ 1 µm/s

- More than an order magnitude speed up of patterning time is possible

- Can field emission mode be used to pattern large contacting leads and pads?
- What size limit is imposed by patterning in field emission mode?

Tunnel gap device electrical dimensions

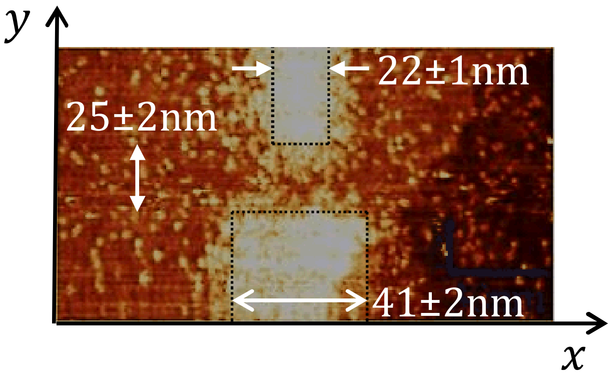

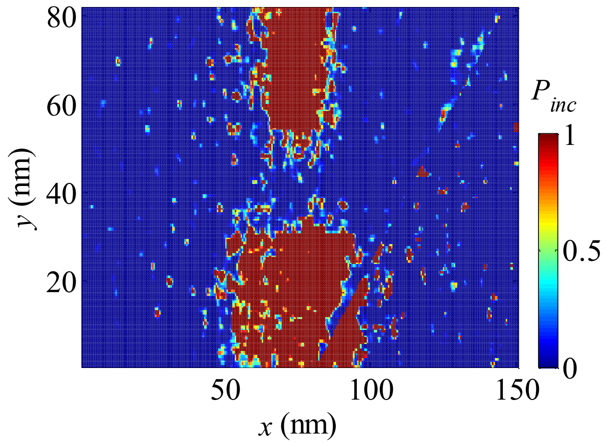

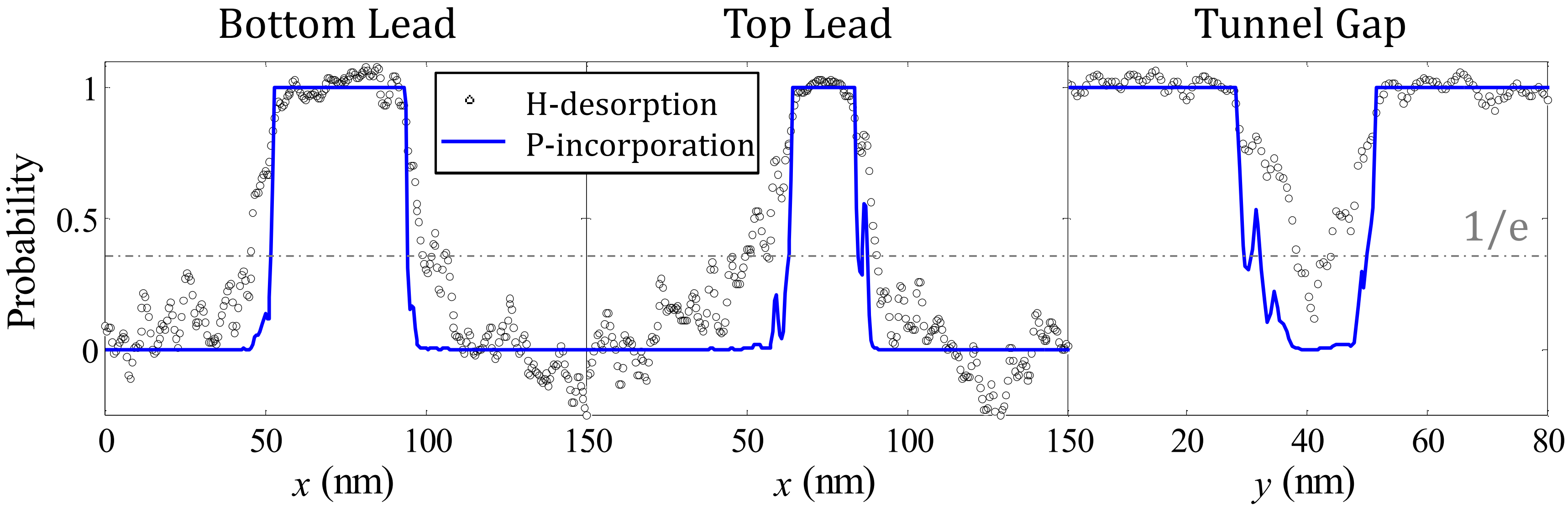

Model of probability of incorporation: Fuechsle (2012)

Rudolph [arXiv 1408.0697]

Scanning cap. Microscopy for STM fab

Original recipe: align to trenched Si marks

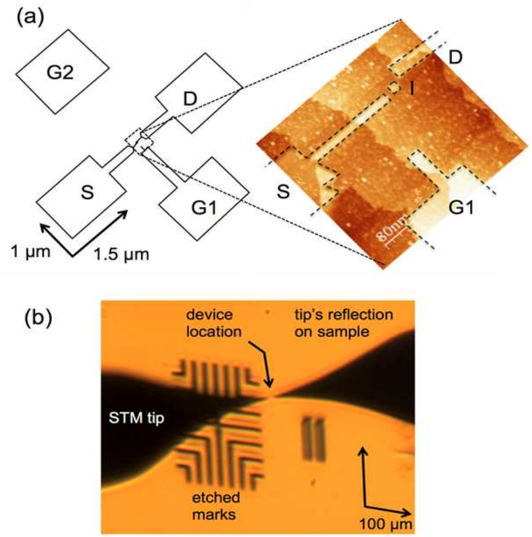

New approach: align to mark after STM fab

Advantage: improved alignment limits & STM fab flexibility

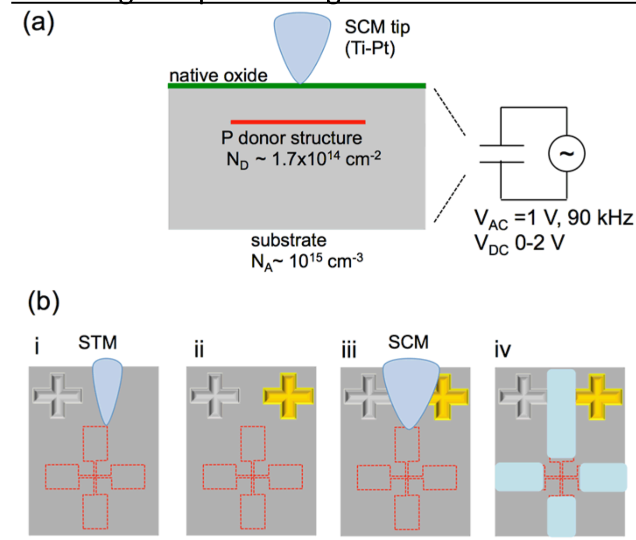

Alignment and post STM fab metrology

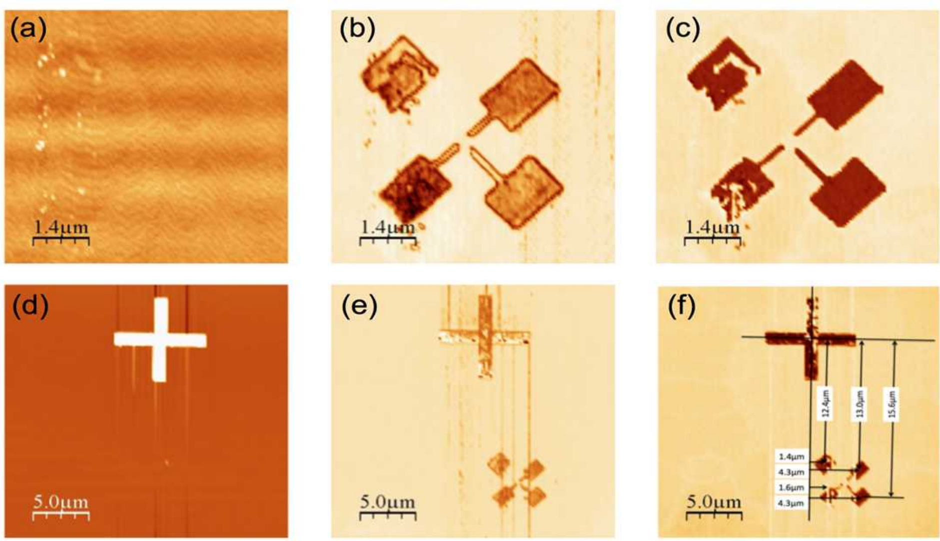

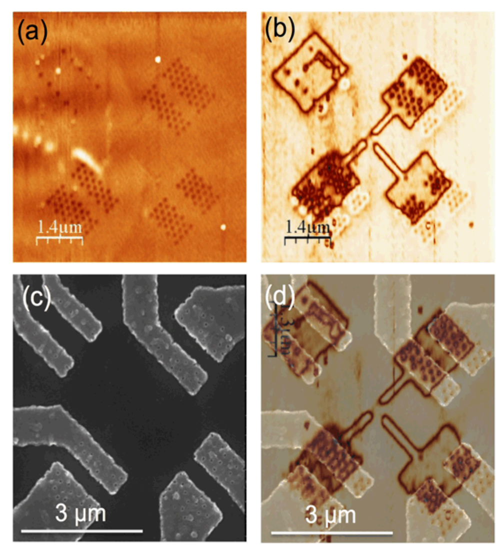

Result:

~300 nm resolution now

10-20 nm possible at RT

Strained silicon-on-insulator (sSOI)

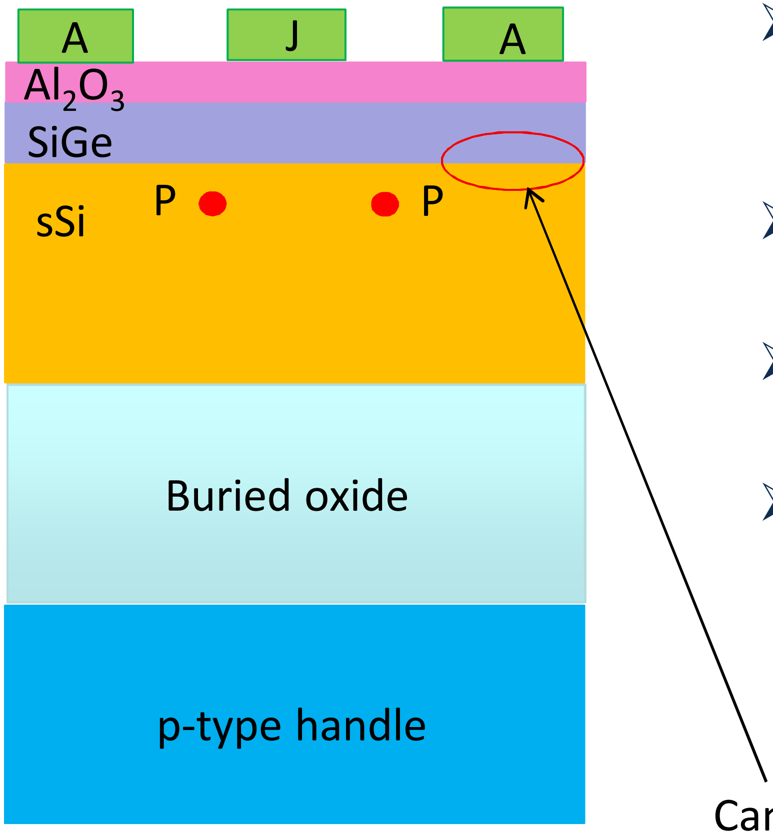

Can we make a good interface?

- sSOI to allow for high temperature clean step [Lee et al., Appl. Surf. Sci. 2012]
- We have ~1% tensile strain in films
- Sharpness of interface is important
- Relaxed SiGe can be used as low temperature capping layer instead of a dielectric

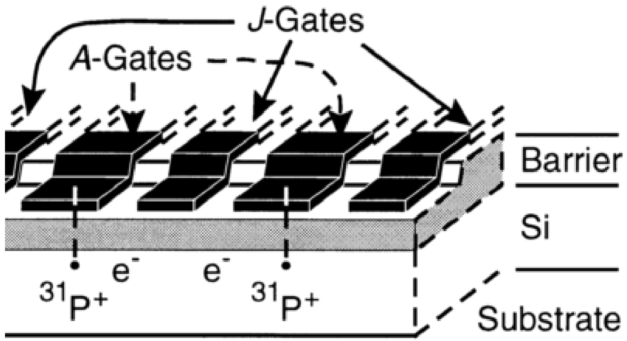

Kane, B., Nature 393, 133 (1998)

AFM / STM of Strained SOI

AFM

Chemical cleaning + no Flash

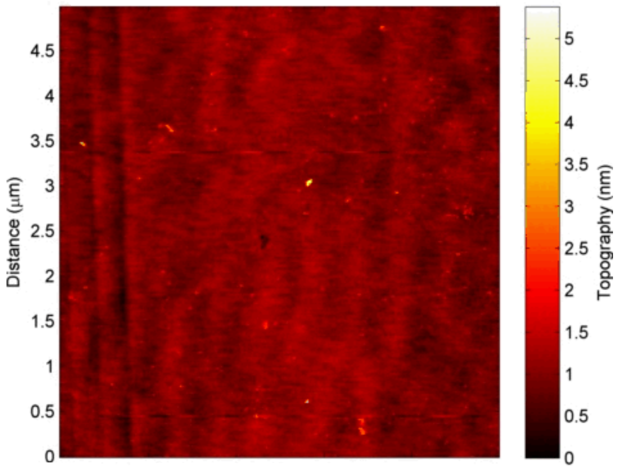

0 Distance [um] 5

RMS roughness = 0.21 nm

Chemical cleaning + Flash Anneal at 940°C

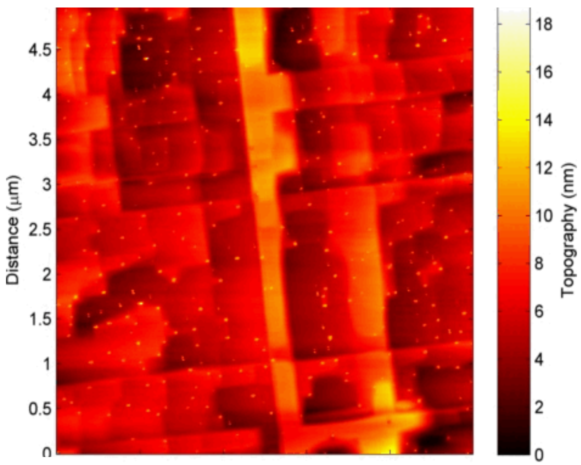

0 Distance [um] 5

RMS roughness = 2.1 nm

STM

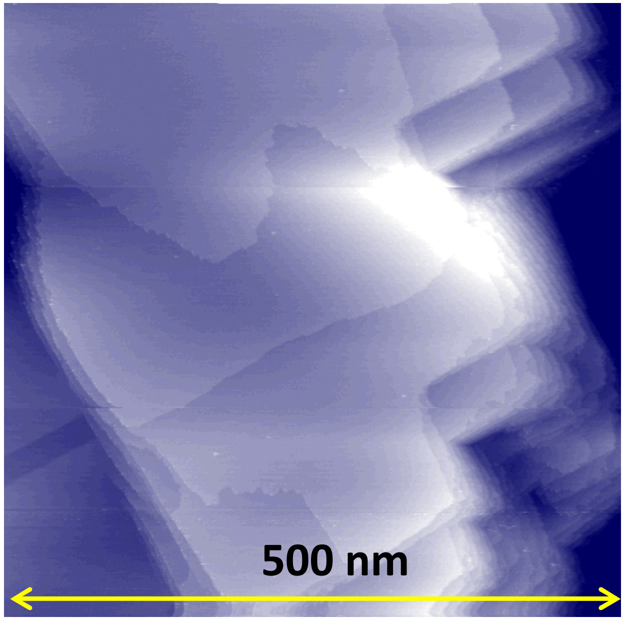

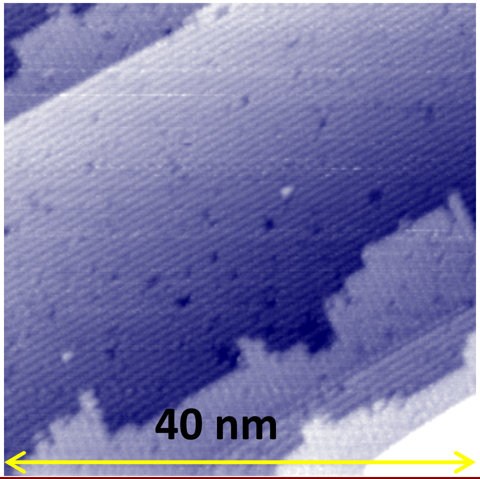

- Surface roughness increases ten-fold once sample is flash-annealed
- Crosshatch patterned island formations, indicating relaxation of strain
- Large terraces form on top of cross-hatch islands a
- Severe step bunching observed on the side of terraces/islands

Hydrogen Lithography on sSOI

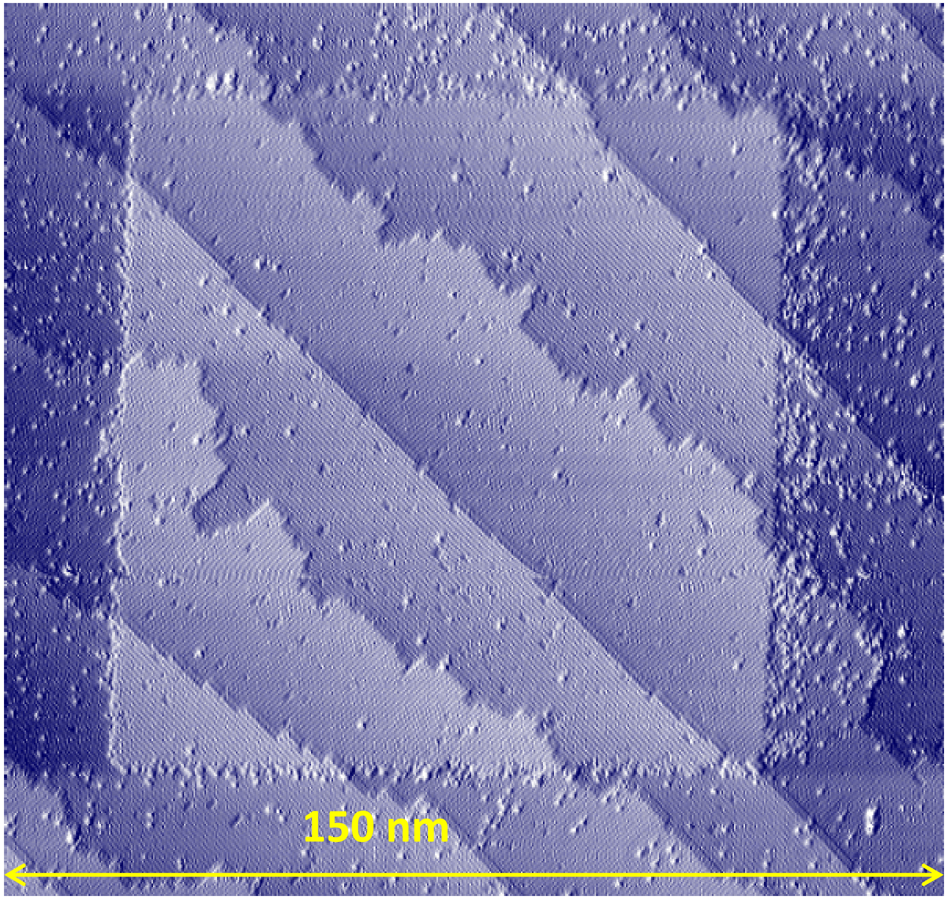

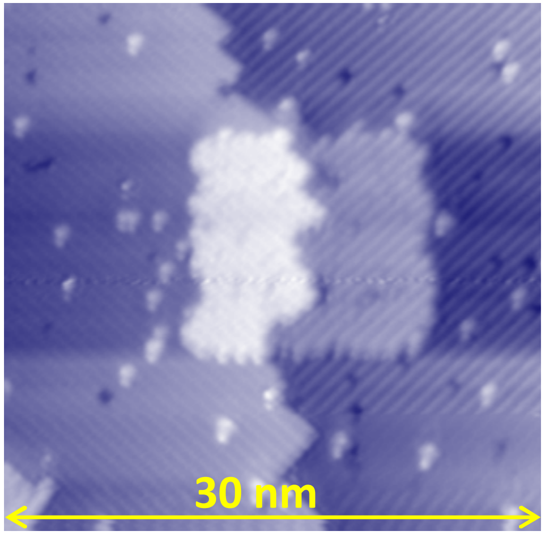

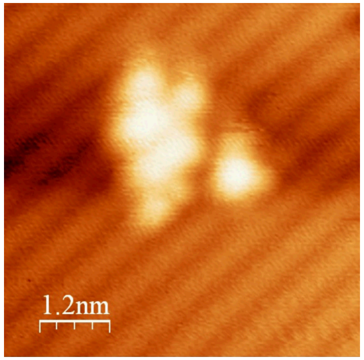

- Surface can be readily hydrogen terminated following same procedure as unstrained Si
- Hydrogen lithography can be done on terraces using typical lithography conditions.

Si Growth on sSOI

Increasing thickness

No heat | 1.4 ML | 3 ML | 34 ML

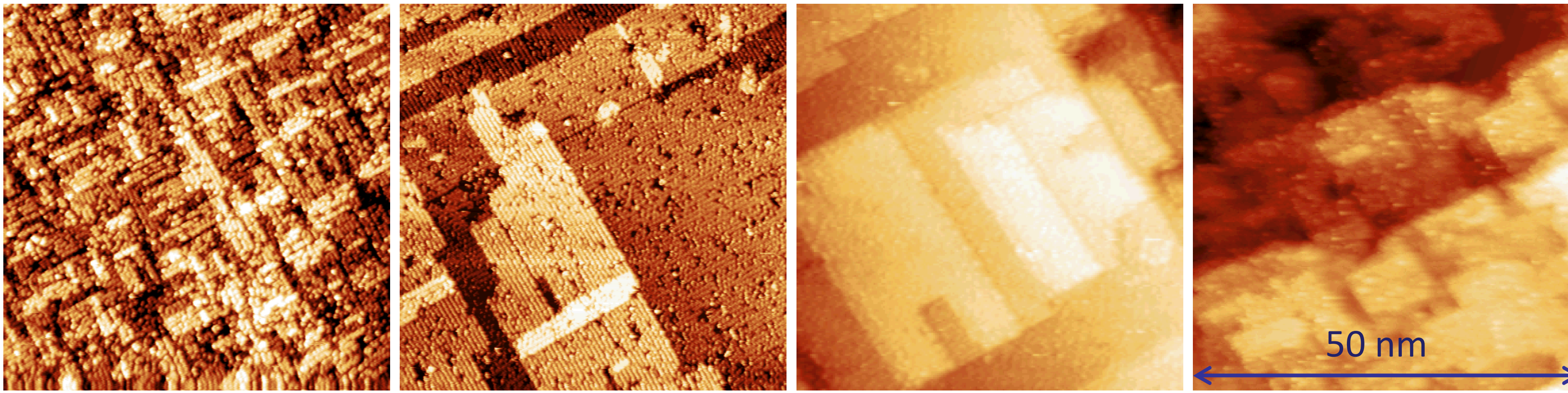

$T_{substrate}$ = ~ 500C

- No heat ➔ the surface is rough ~ 5 Å
- With heat, there is more order on the surface: 2-D islands form
- With increasing thickness, larger islands form, and further, there is an increase in island density

AFM of 23.4 nm Si growth on sSOI

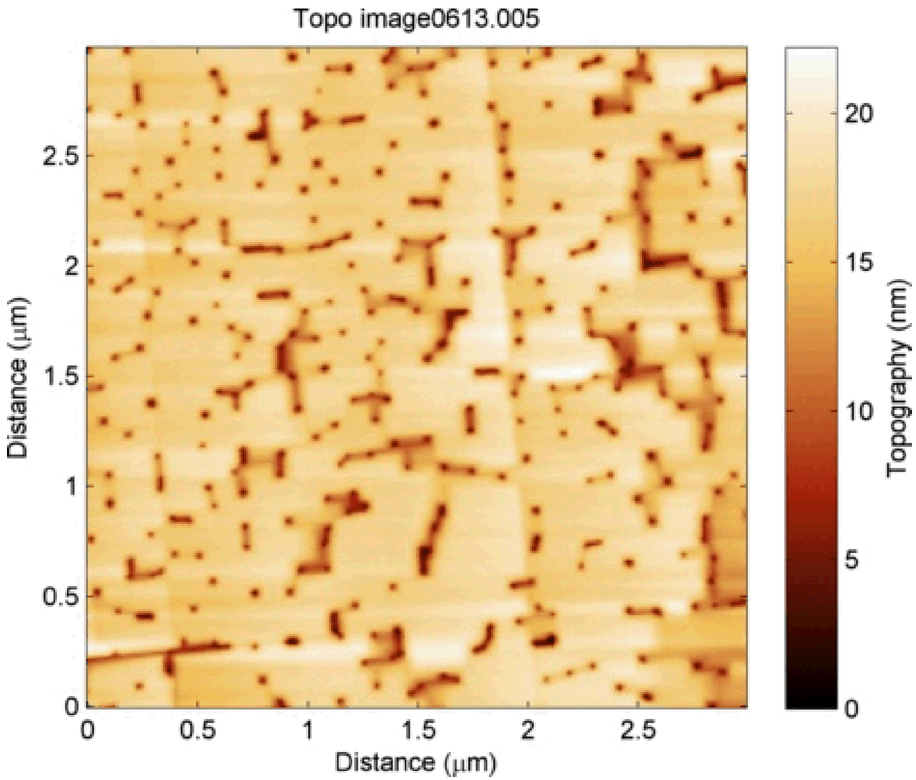

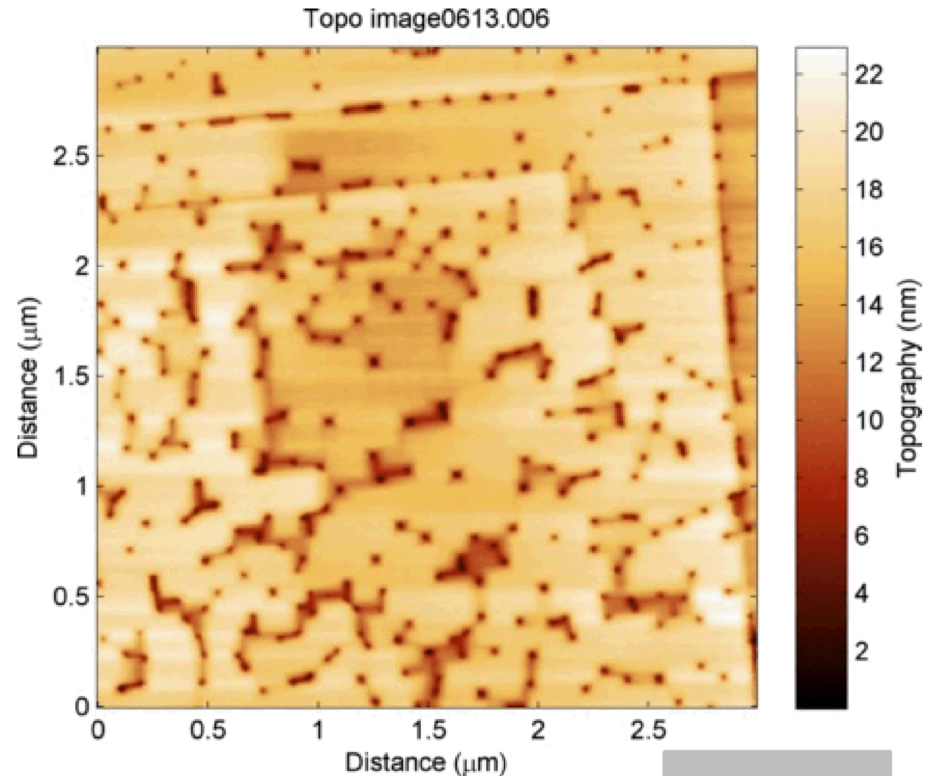

Roughness = 2.63 nm

Roughness = 2.93 nm

T_{sub} = 600C

Smooth surfaces (sub nm roughness) with pits
Pits possibly due to carbon contamination
Might be able to recover smooth surface

STM of 5.85 nm Si/sSOI

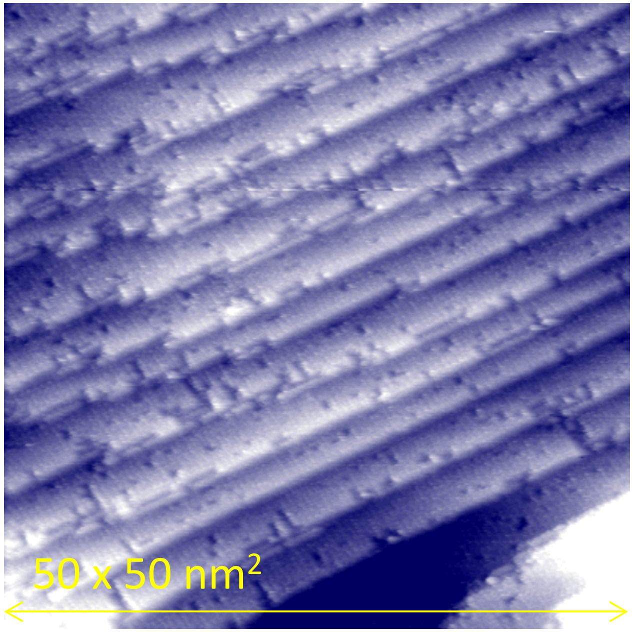

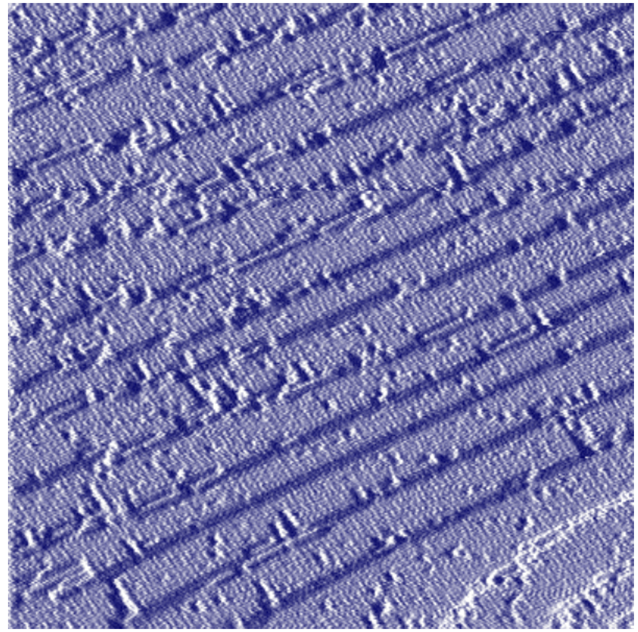

T_{sub} = 560C

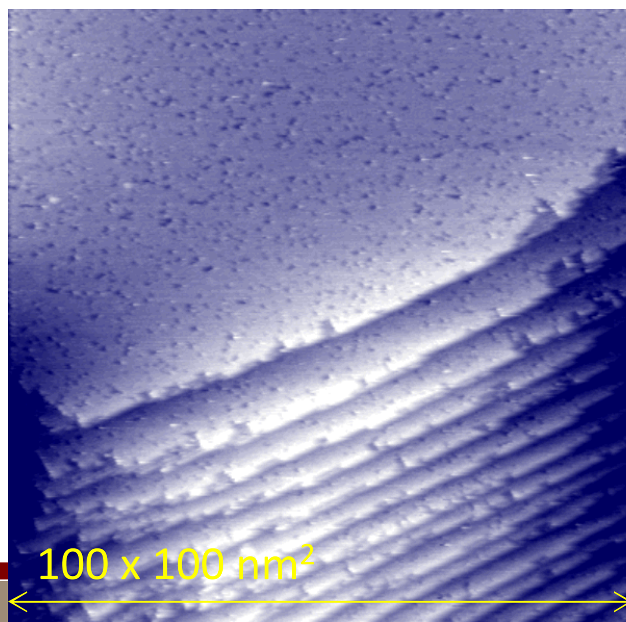

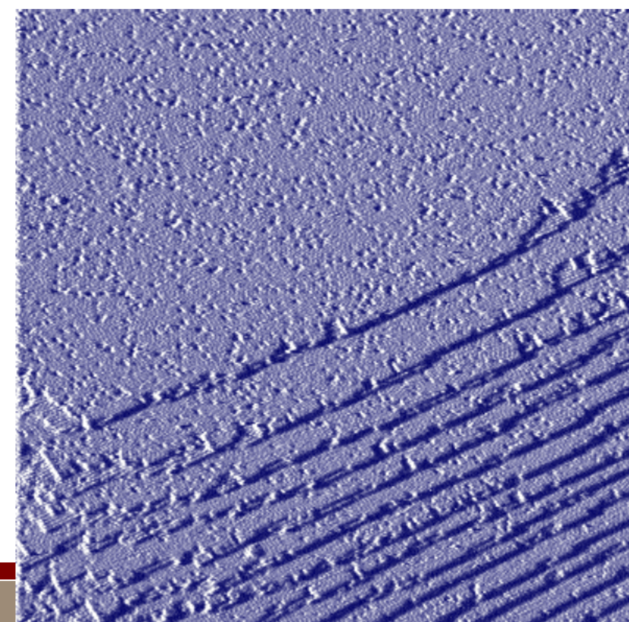

SiGe Growth (~20 % Ge) on sSOI

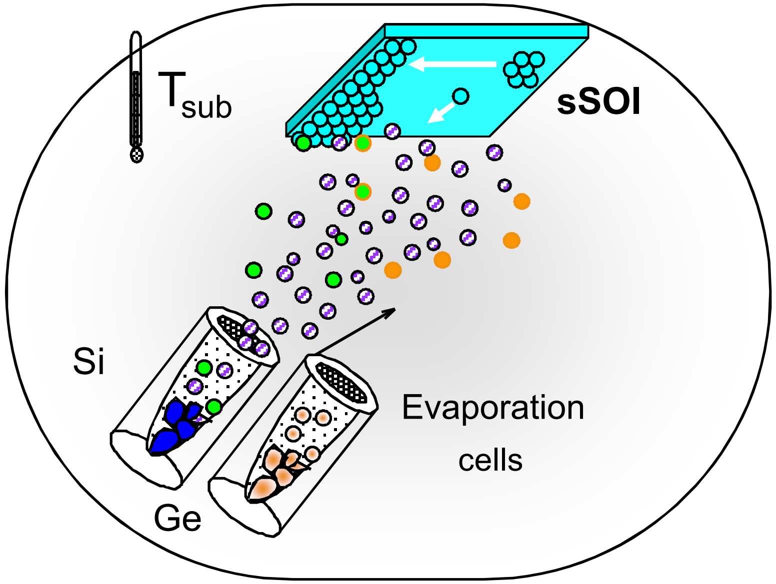

- Sample preparation
  - Evaporation of Si and Ge on Si(001);
  - Si flux is 0.032Å/s and Ge flux is ~ 0.006 Å/s
  - Substrate kept at ~ 500 - 550C during deposition;
- Scanning tunneling microscopy (STM)
  - Sample imaged at room temperature.

20% SiGe is approximately lattice matched with the sSOI

Different Thickness of SiGe (~20 % Ge) on sSOI

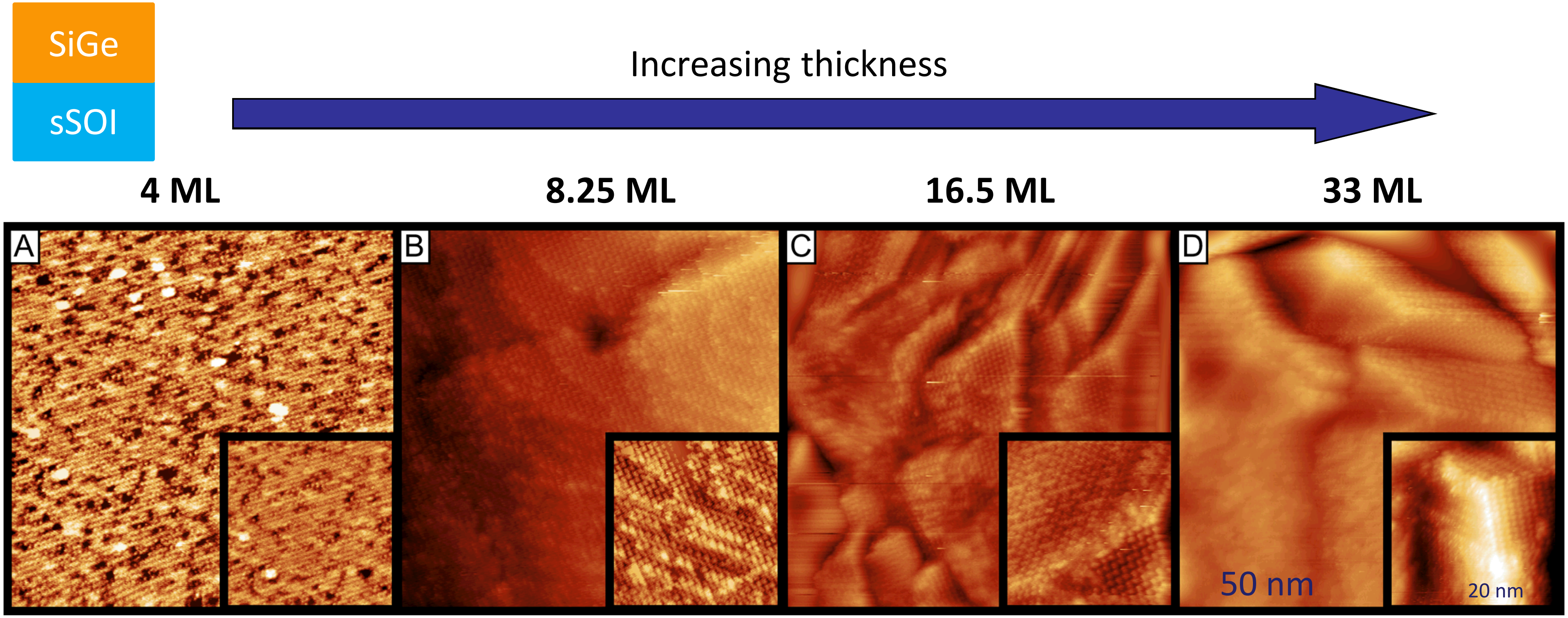

- At low coverage, observation of dimer row reconstruction, although defects in reconstruction is relatively high
- With increasing thickness, shallow 3D islands start to form (~2-3 nm peak to valley)
- MBE of unstrained SiGe on Si reported flat for these conditions [Bean et al., JVST A 2(1986)]
- TEM shows defect free interface
- Next: make devices and work on smoother growth conditions

Summary

Silicon P donor qubit w/ self-aligned implant

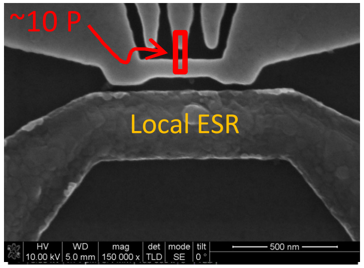

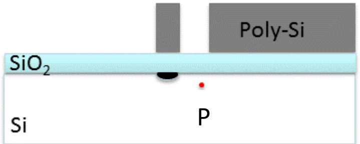

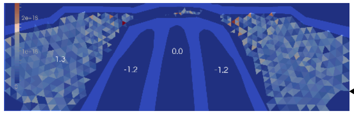

← & Si QD simulation

Spin read-out, T1 of Sb &Rabi oscillations

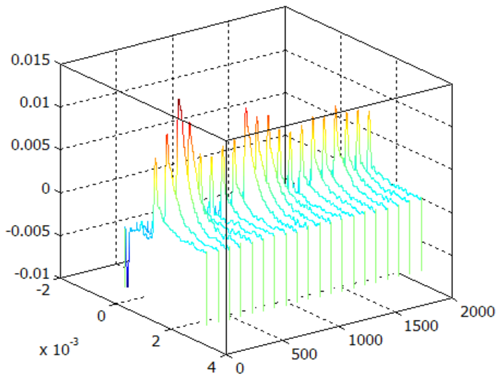

Single Sb^+ implant map (50 keV)

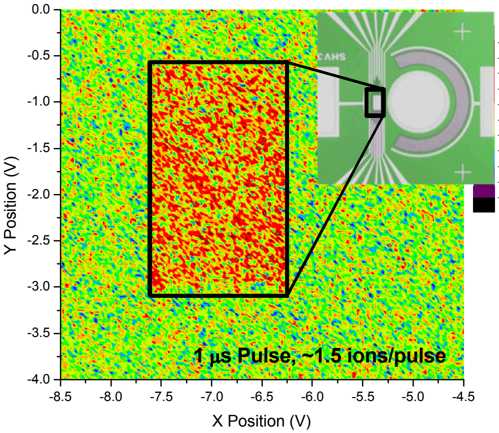

SiGe/ssOI STM assisted nanofabrication

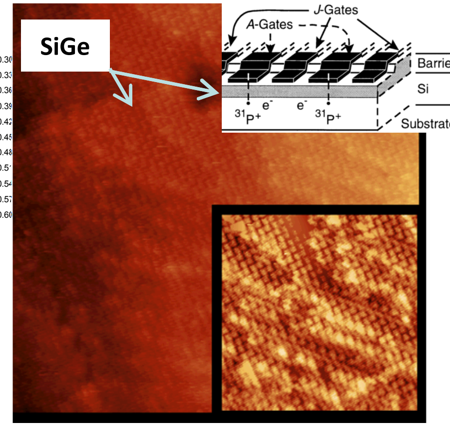

Field emission STM tunnel barrier

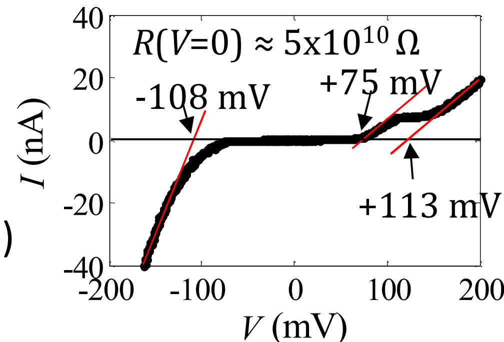

- Local ESR demonstrated in poly-Si process flow
- Dot behavior is regular in newer designs
  - Device modeling agrees reasonably well with measured QDs
- We're looking at surface J-gate approach for two qubit path (implant or STM)
- Single ion implant capability integrated w. similar process flow
- Remote sensed D-QD and D-QD-D structures for immediate measurements of donor coupling to surface
- STM assisted tunnel barrier fabricated (examining limits of field emission writing mode) & SCM alignment
- SiGe growth on sSOI in STM system for STM path for 2 qubit

Posters: Bishop, Bussmann, Witzel (gap protection and DD)

QIST team & external connections

- QIST contributors at SNL

  Qubit fab: M. Busse, J. Dominguez, T. Pluym, B. Silva, G. Ten Eyck, J. Wendt, S. Wolfley

  Qubit control & measurement: N. Bishop, S. Carr, M. Curry, S. Eley, T. England, M. Lilly, T.-M. Lu, D. Luhman, K. Nguyen, M. Rudolph, P. Sharma, A. Shirkhorshidian, M. Singh, L. Tracy, M. Wanke

  Advanced fabrication (two qubit): E. Bielejec, E. Bussmann, E. Garratt, A. MacDonald, E. Langlois, B. McWatters, S. Miller, S. Misra, D. Perry, D. Scrymgeour, D. Serkland, G. Subramanian, E. Yitamben

  Device modeling: J. Gamble, T. Jacobson, R. Muller, E. Nielsen, I. Montano, W. Witzel, R. Young

- Joint research efforts with external community:
  - Australian Centre for Quantum Computing and Communication Technology (D. Jamieson, A. Dzurak, A. Morello, M. Simmons, L. Hollenberg)
  - Princeton University (S. Lyon)
  - NIST (N. Zimmerman)
  - U. Maryland (S. Das Sarma)
  - National Research Council (A. Sachrajda)
  - U. Sherbrooke (M. Pioro-Ladriere)
  - Purdue University (G. Klimeck & R. Rahman)
  - U. New Mexico (I. Deutsch, P. Zarkesh-Ha)
  - U. Wisconsin (M. Eriksson)
  - University College London (J. Morton, S. Simmons)

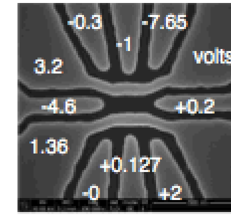

QD-D anti-crossings

Region of interest

Sweeping CP vs AG reveals CP-side D. Sweeping LISO/RISO reveals ISO-side D. The other side donors always have very similar slopes to the QD.

QD charging energy ~4.8 meV

CPL-side D

CS-side D

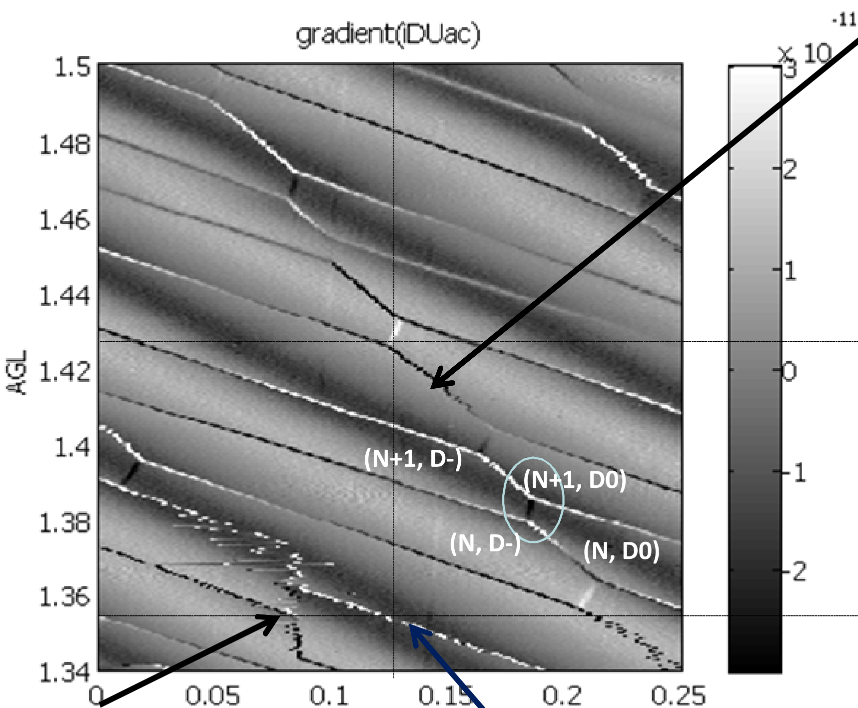

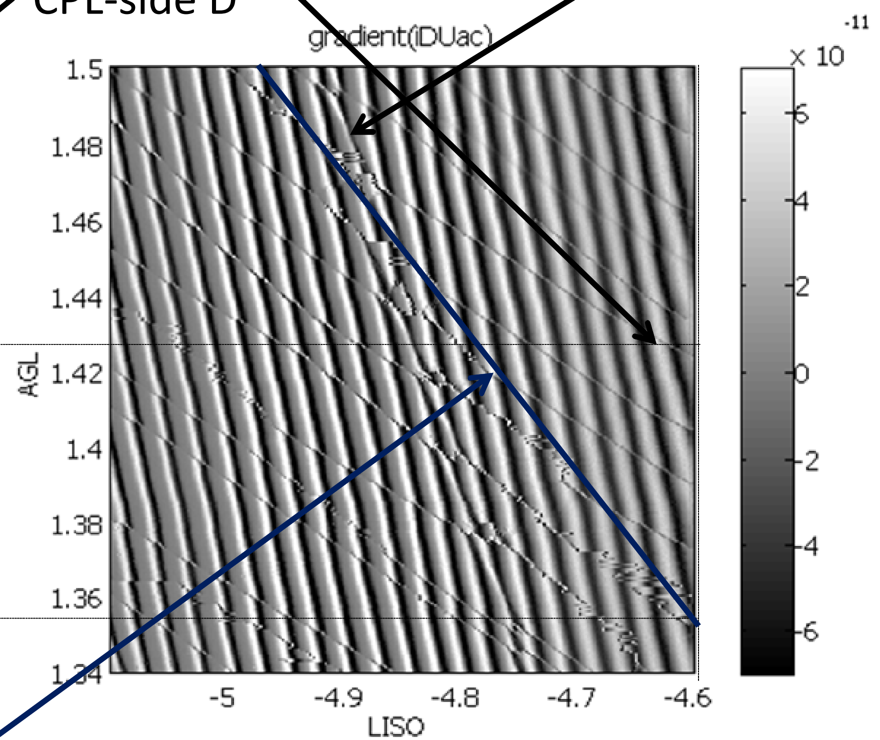

D-D transition?

ISO-side D

RISO = LISO + 4.8 V

Pulsing from a fixed point to a variable wait point (two level)

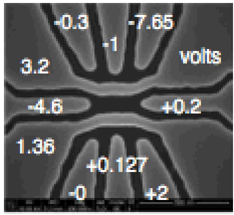

20140731T110803
B = 0 mT
load = 1 us;
wait = 9 us

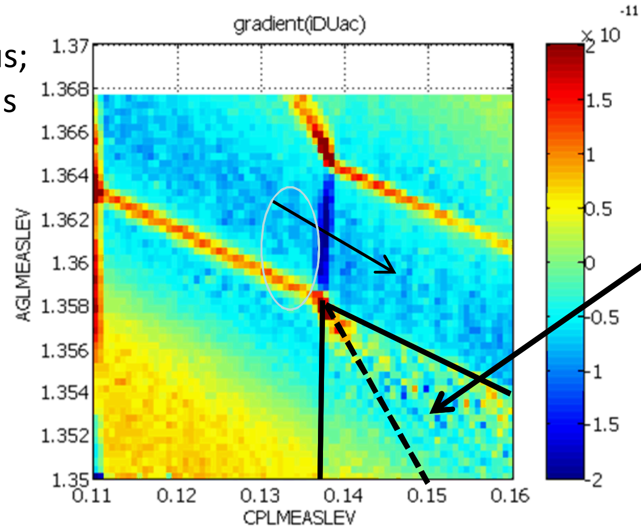

No doubling: hysteretic transition

20140731T115129
B = 0 mT
load = 1 us;
wait = 9 us

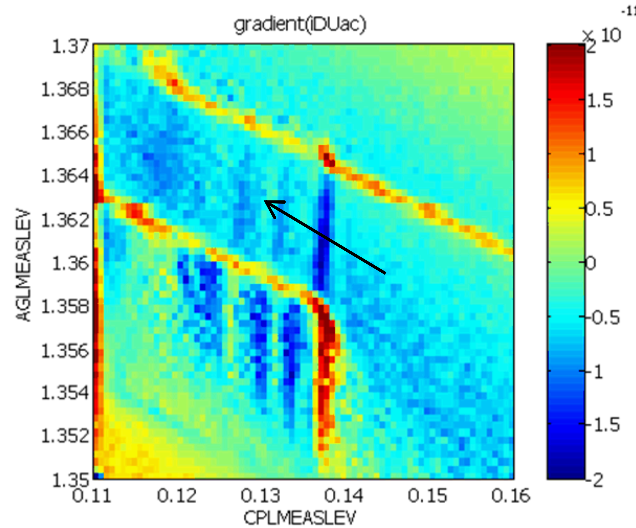

20140731T141508
B = 50 mT
load = 1 us;
wait = 9 us

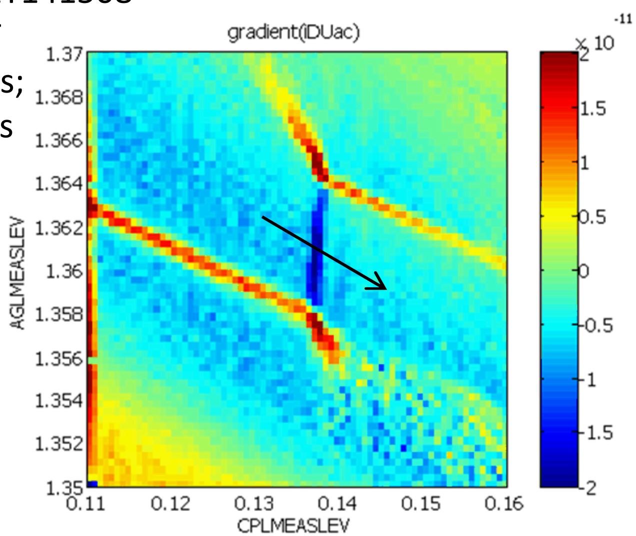

20140731T131001
B = 50 mT
load = 1 us;
wait = 9 us

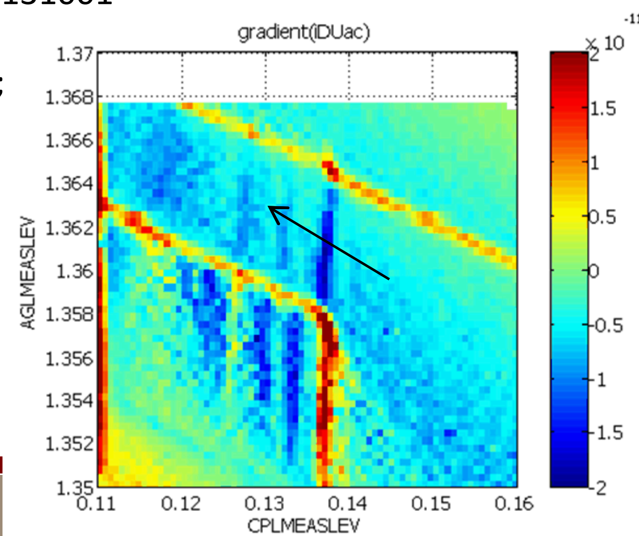

Characterize Adiabatic Sweeps:

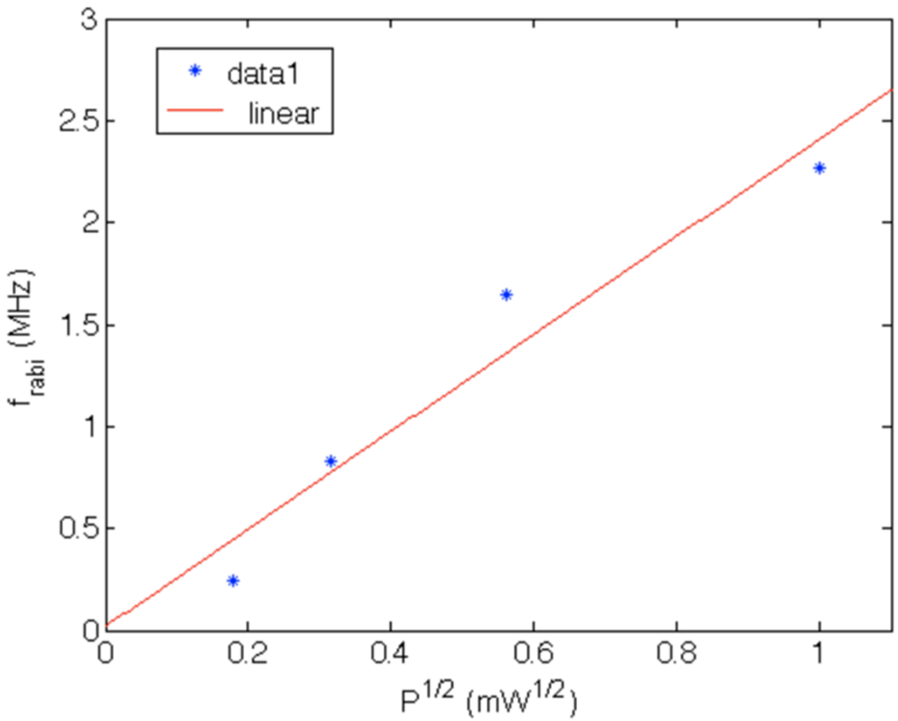

B_1~0.08 mT @0 dBm

Attenuation in lines 20-25 dB

$F_{rabi}=2.39*P^{1/2}-0.018$

For 6 dBm f_{rabi}~4.75 MHz (B_1~0.17 mT)

Previous measurement by DRL~5 MHz

$$\frac{\pi^2 f_r^2}{\Delta\nu / t_{pulse}}$$ @ t_{pulse}=10 us

-15 dBm	0.236
-10 dBm	2.75
-5 dBm	10.7
0 dBm	20.3

For 9 dBm f_{rabi}~6.72 MHz (B_1~0.24 mT)

$f_{rabi\ NMR} \geq 4$ kHz

$$\frac{\pi^2 f_r^2}{\Delta\nu / t_{pulse}} = 1.58$$ @ t_{pulse}=10 ms

The MOS interface

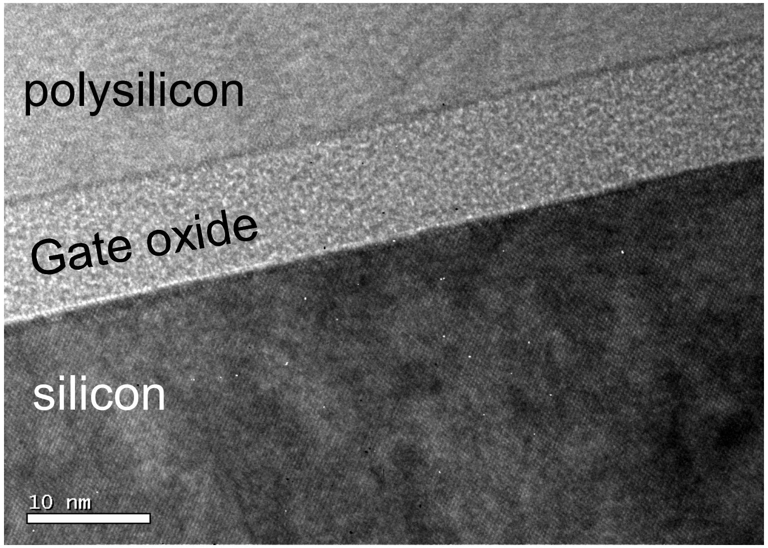

Defects

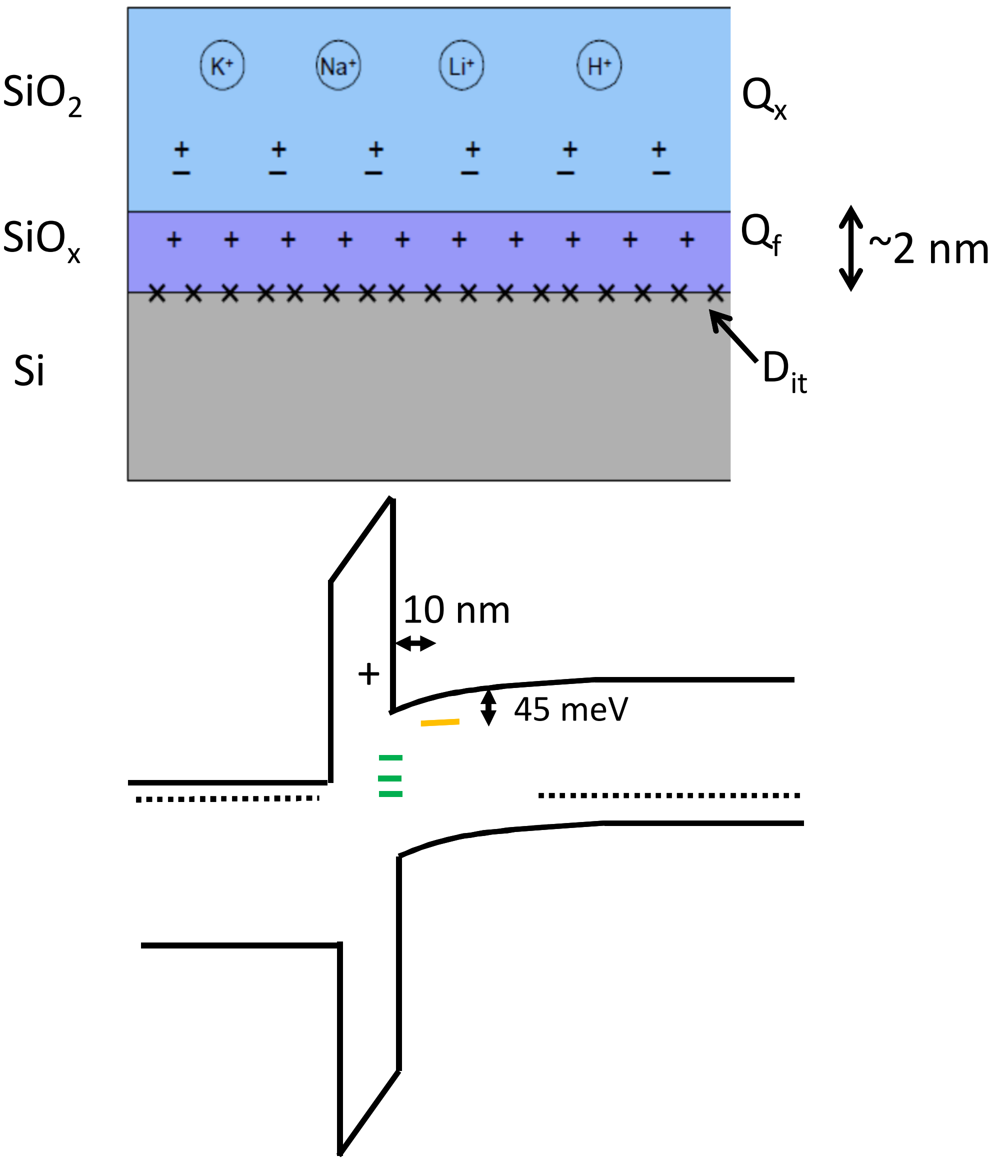

Room temperature picture

- D_{it} Interface traps and border traps within a "tunneling" distance of interface
- Q_f Fixed charge deeper in oxide

- What is relevant at low temperature?

Oxide defect densities

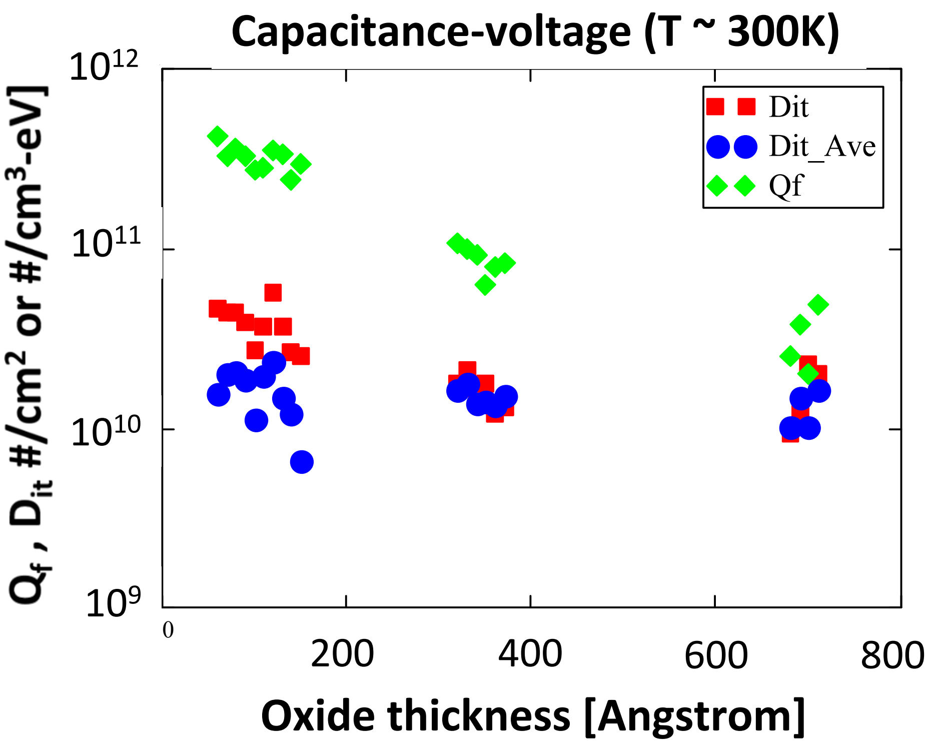

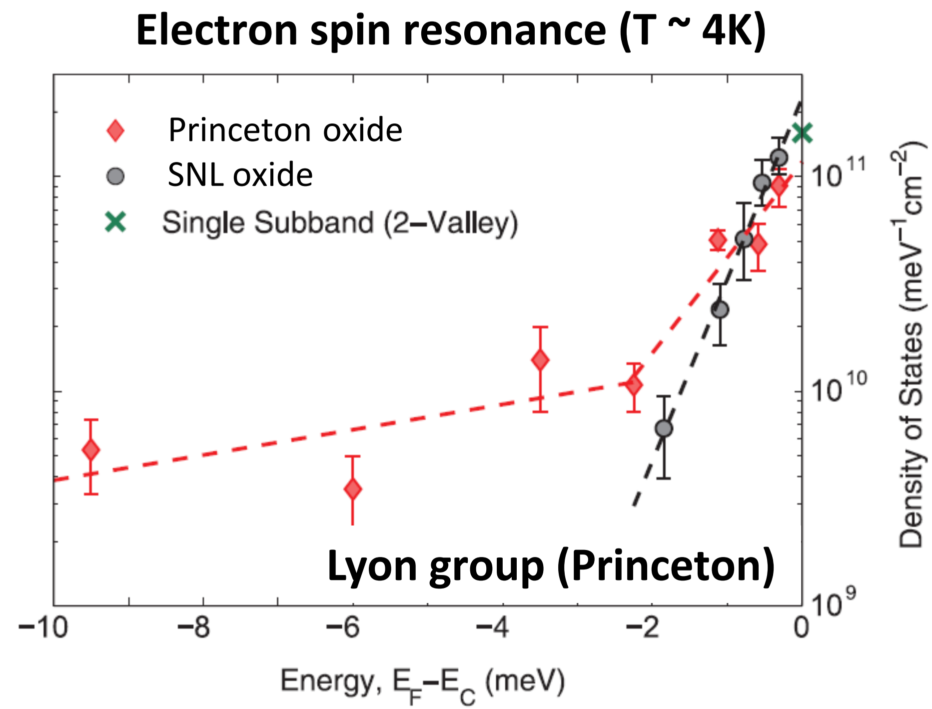

5,000 cm² / V-s < mobility < 15,000 cm² / V-s

Jock et al., APL 2012

18 dBm: 10 Repeats

T085233

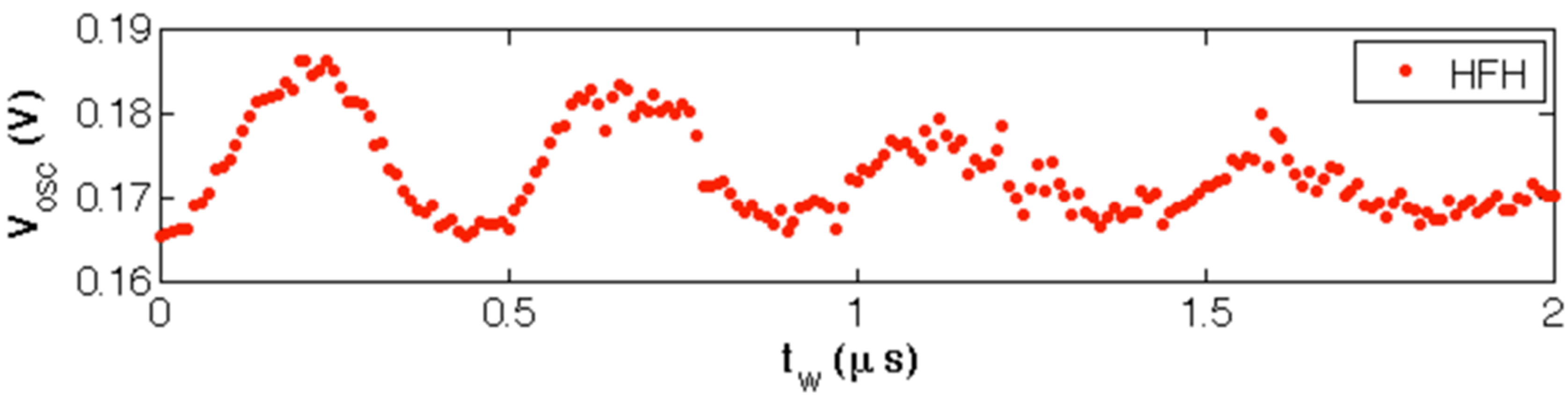

This is an example with 10 repeats and 128 averages per repeat. For all the data the total number of averages isn't simply 128*10 since for some values of t_w the sample was in HFL or MF and those data were rejected. Given that caveat, this is a factor of 15 or so less in number of total averages than Khoi's Rabi data.

All Rabi data is taken for HFH

V_{osc} are the max spin bump values

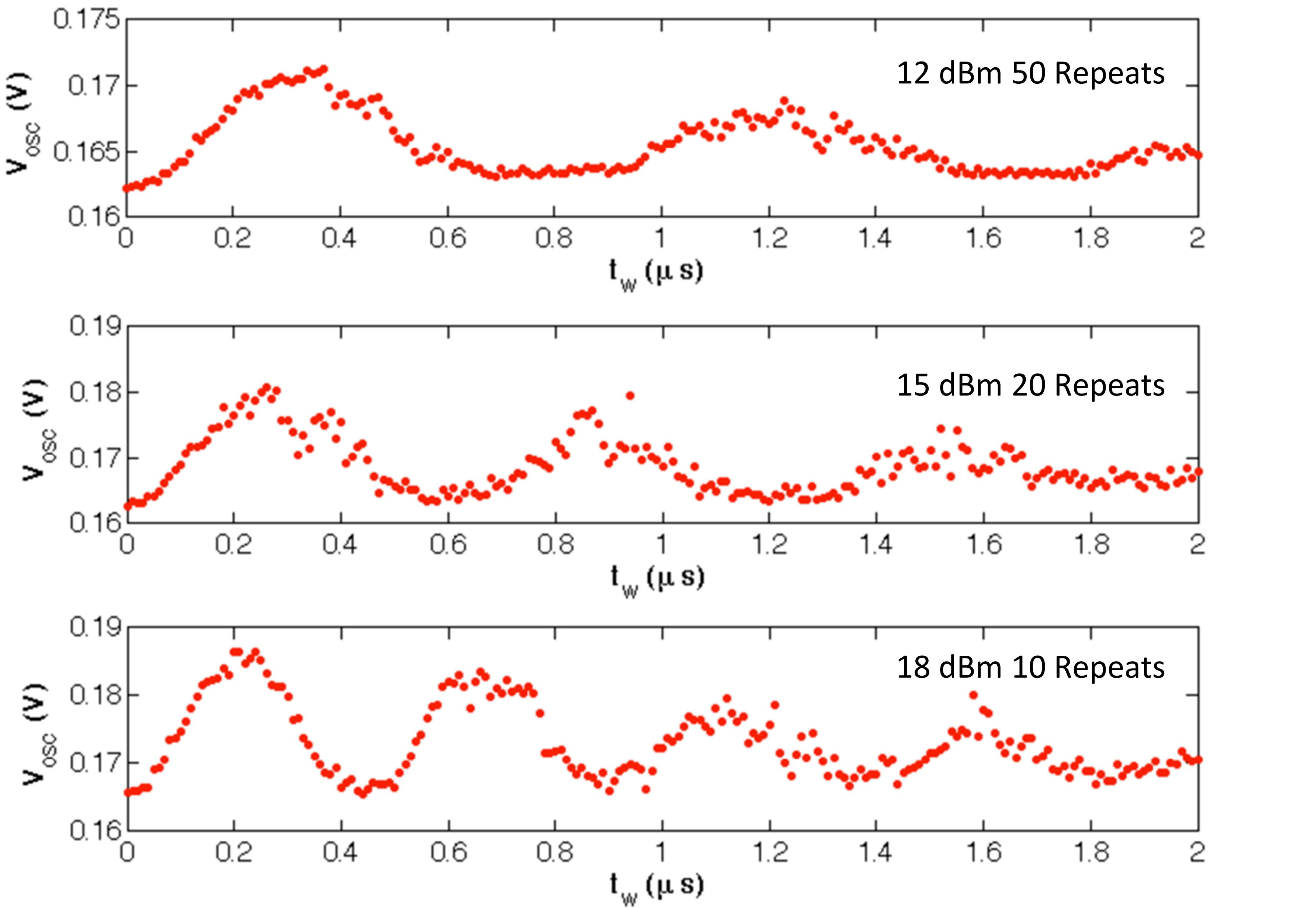

12 dBm 50 Repeats
15 dBm 20 Repeats
18 dBm 10 Repeats
V_{osc} (V)
t_w (μ s)
0.175
0.17
0.165
0.16
0.19
0.18
0
0.2
0.4
0.6
0.8
1
1.2
1.4
1.6
1.8
2

Incomplete pulsed X rotations due to spin bath diffusion

- 128 averages per trace
- 150 repeats
- Fixed frequency (36.459 GHz)

- For a fixed rotation (~pi pulse) time:
    - sometimes the spin signal is small, sometimes large

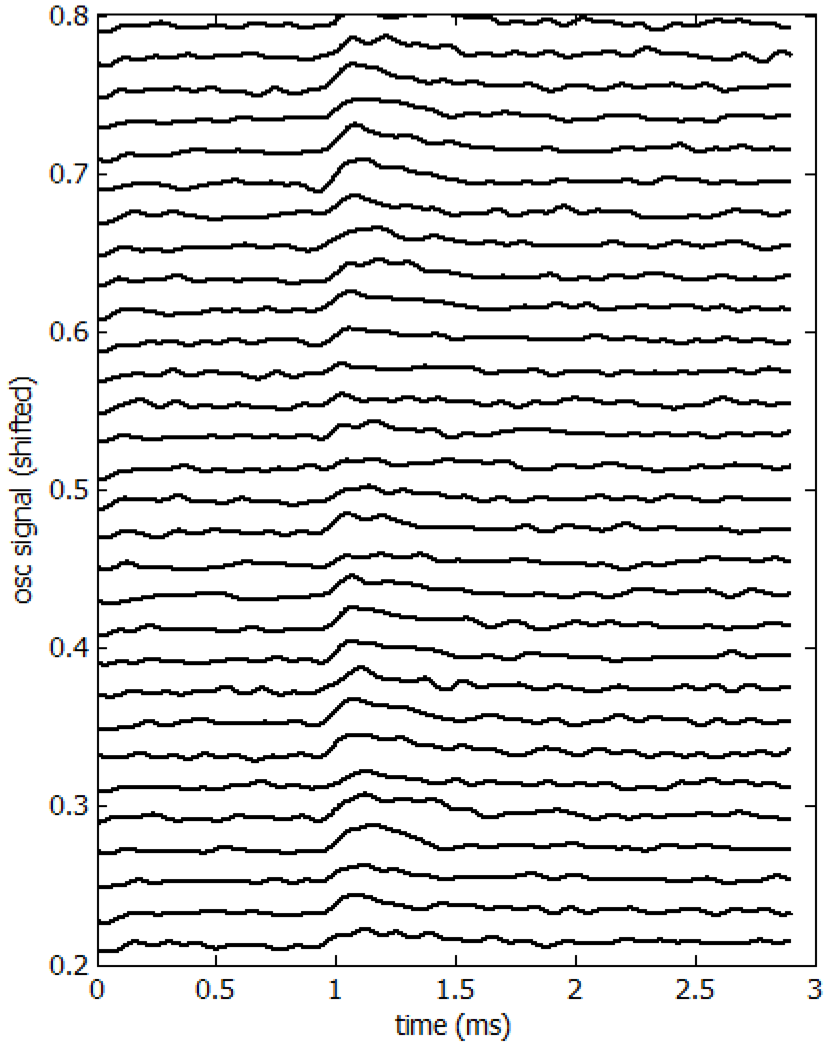

Lilly

STM of 5.85 nm Si/sSOI

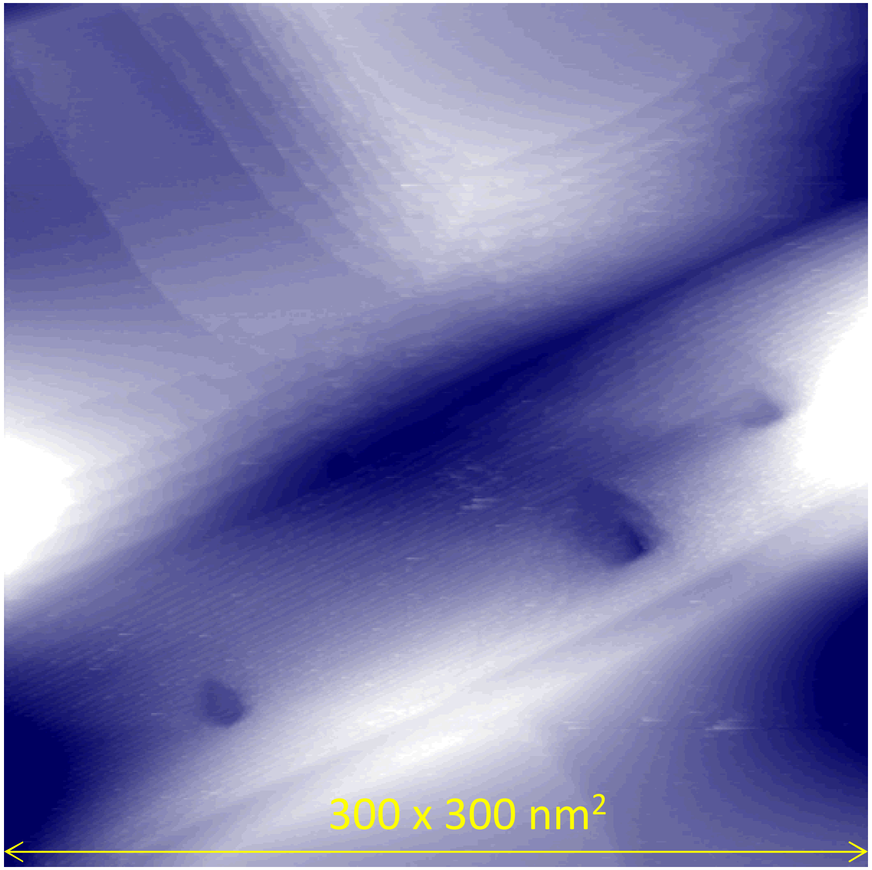

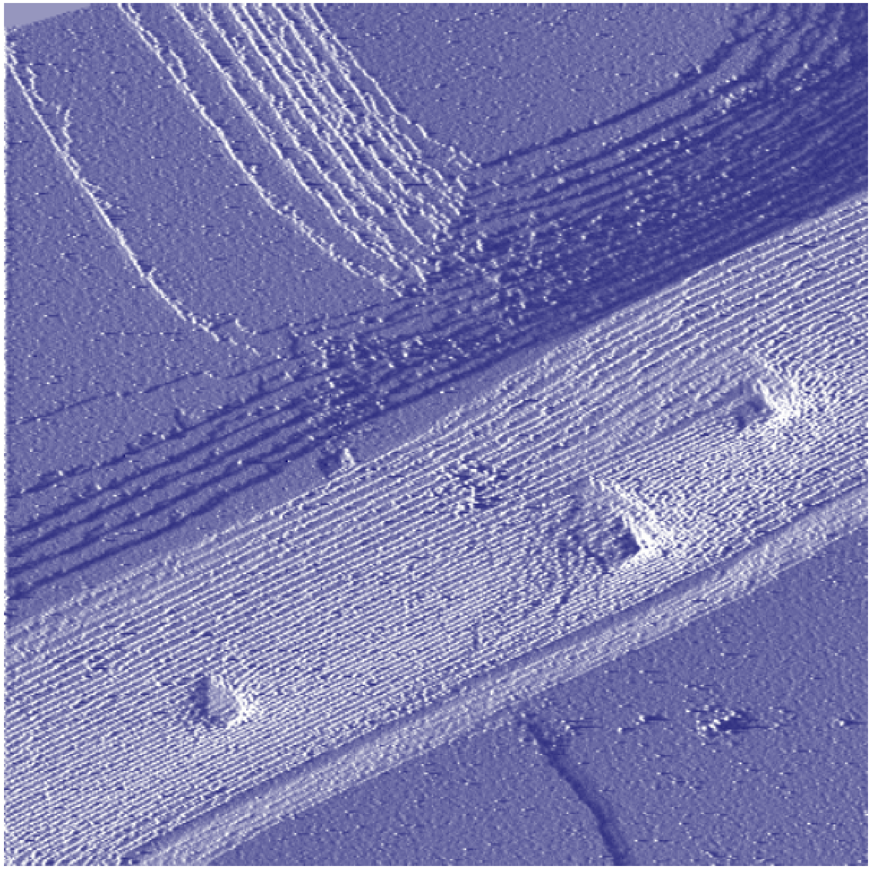

T_{sub} = 585C

Effective mass and tight-binding agree: tunnel coupling is very sensitive to position

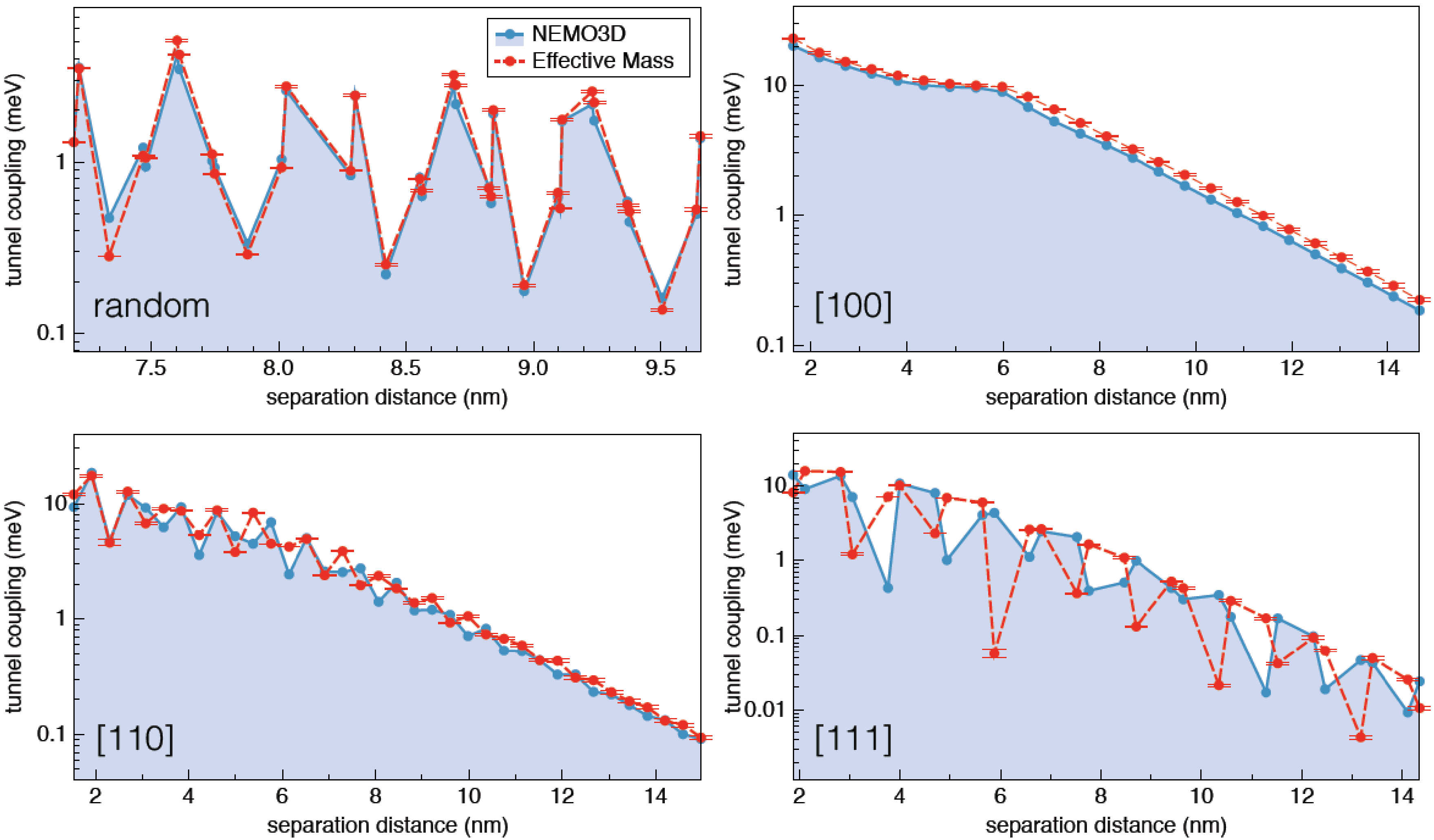

New central cell correction for EMT.